

FINAL REPORT

Mechanochemical Preparation of Organic Nitro Compounds

SERDP Project WP-2748

MAY 2018

Edward Dreizin
Oleg Shlomo Lagoviyer
Mirko Schoenitz
New Jersey Institute of Technology

Distribution Statement A

This document has been cleared for public release



Page Intentionally Left Blank

This report was prepared under contract to the Department of Defense Strategic Environmental Research and Development Program (SERDP). The publication of this report does not indicate endorsement by the Department of Defense, nor should the contents be construed as reflecting the official policy or position of the Department of Defense. Reference herein to any specific commercial product, process, or service by trade name, trademark, manufacturer, or otherwise, does not necessarily constitute or imply its endorsement, recommendation, or favoring by the Department of Defense.

Page Intentionally Left Blank

REPORT DOCUMENTATION PAGE

Form Approved
OMB No. 0704-0188

The public reporting burden for this collection of information is estimated to average 1 hour per response, including the time for reviewing instructions, searching existing data sources, gathering and maintaining the data needed, and completing and reviewing the collection of information. Send comments regarding this burden estimate or any other aspect of this collection of information, including suggestions for reducing the burden, to Department of Defense, Washington Headquarters Services, Directorate for Information Operations and Reports (0704-0188), 1215 Jefferson Davis Highway, Suite 1204, Arlington, VA 22202-4302. Respondents should be aware that notwithstanding any other provision of law, no person shall be subject to any penalty for failing to comply with a collection of information if it does not display a currently valid OMB control number.
PLEASE DO NOT RETURN YOUR FORM TO THE ABOVE ADDRESS.

1. REPORT DATE (DD-MM-YYYY) 05/04/2018		2. REPORT TYPE SERDP Final Report		3. DATES COVERED (From - To) 2/14/2017 - 2/13/2019	
4. TITLE AND SUBTITLE MECHANOCHEMICAL PREPARATION OF ORGANIC NITRO COMPOUNDS				5a. CONTRACT NUMBER Contract: W912HQ-17-P-0009	
				5b. GRANT NUMBER	
				5c. PROGRAM ELEMENT NUMBER	
6. AUTHOR(S) Edward L. Dreizin Oleg Shlomo Lagoviyer Mirko Schoenitz				5d. PROJECT NUMBER WP-2748	
				5e. TASK NUMBER	
				5f. WORK UNIT NUMBER	
7. PERFORMING ORGANIZATION NAME(S) AND ADDRESS(ES) New Jersey Institute of Technology University Heights Newark, NJ 07102				8. PERFORMING ORGANIZATION REPORT NUMBER WP-2748	
9. SPONSORING/MONITORING AGENCY NAME(S) AND ADDRESS(ES) Strategic Environmental Research and Development Program 4800 Mark Center Drive, Suite 17D03 Alexandria, VA 22350-3605				10. SPONSOR/MONITOR'S ACRONYM(S) SERDP	
				11. SPONSOR/MONITOR'S REPORT NUMBER(S) WP-2748	
12. DISTRIBUTION/AVAILABILITY STATEMENT Distribution A; unlimited public release					
13. SUPPLEMENTARY NOTES					
14. ABSTRACT Aromatic compounds such as toluene are commercially nitrated using a combination of nitric acid with other strong acids. This process relies on the use of highly corrosive chemicals and generates environmentally harmful waste, which is difficult to handle and dispose of. In this study aromatic nitration using solvent-free mechanochemical processing of environmentally benign precursors has been achieved and investigated. Mononitrotoluene (MNT) was synthesized by milling toluene with sodium nitrate and molybdenum trioxide as a catalyst.					
15. SUBJECT TERMS aromatic compounds, Mechanochemical Preparation, Organic Nitro Compounds, Mononitrotoluene					
16. SECURITY CLASSIFICATION OF:			17. LIMITATION OF ABSTRACT	18. NUMBER OF PAGES	19a. NAME OF RESPONSIBLE PERSON
a. REPORT	b. ABSTRACT	c. THIS PAGE			Edward Dreizin
UNCLASS	UNCLASS	UNCLASS	UNCLASS	59	19b. TELEPHONE NUMBER (Include area code) 973-596-5751

Page Intentionally Left Blank

ABSTRACT

Aromatic compounds such as toluene are commercially nitrated using a combination of nitric acid with other strong acids. This process relies on the use of highly corrosive chemicals and generates environmentally harmful waste, which is difficult to handle and dispose of. In this study aromatic nitration using solvent-free mechanochemical processing of environmentally benign precursors has been achieved and investigated. Mononitrotoluene (MNT) was synthesized by milling toluene with sodium nitrate and molybdenum trioxide as a catalyst. Several parameters affecting the desired product yield and selectivity were identified and varied. MNT yields in excess of 60% have been achieved in different tests. The desired product yield and selectivity were found to depend on the ratios of the reactants and the catalyst. A parametric study addressed the effects of milling time, temperature, milling media, and catalyst additives on the MNT yield and on the formation of various byproducts. Toluene conversion as a function of milling time exhibited a maximum, which occurred earlier for smaller milling balls. Milling temperature had only a weak effect on MNT formation, but affected the formation of other aromatic byproducts. Replacing various fractions of MoO_3 with fumed silica led to an increased yield of MNT for up to 30% of silica. The yield dropped when higher percentages of MoO_3 were replaced. The degree of refinement of MoO_3 attained in the mill has been quantified by measuring the surface area of the inorganic fraction of the milled material. The surface measurements were correlated with the product yield. Feasibility of secondary nitration for toluene as well as of mechanochemical nitration of anisole and naphthalene has also been shown experimentally.

Contents

ABSTRACT	1
CHAPTER 1: LITERATURE REVIEW	4
1.1 Introduction: Nitration Reactions	4
1.2 Shortcomings of Common Nitration Methods.....	4
1.3 Improved Nitration Methods.....	5
1.4 Mechanochemically Induced Nitration Reactions	10
1.4.1 Mechanochemical Reactions	10
1.4.2 Mechanochemical Nitration of Organic Compounds	14
CHAPTER 2: MECHANOCHEMICAL NITRATION OF TOLUENE: FEASIBILITY 17	
2.1 Introduction.....	17
2.2 Experimental.....	18
2.3 Results.....	21
2.3.1 Formation of Mononitrotoluene with MoO ₃ as a Catalyst.....	21
2.3.2 Parameters Affecting the Product Yield	22
2.4 Discussion.....	28
2.5 Conclusions.....	28
CHAPTER 3: EFFECT OF PROCESS PARAMETERS ON MECHANOCHEMICAL NITRATION OF TOLUENE	29
3.1 Introduction.....	29
3.2 Experimental.....	30
3.2.1 Sample Preparation	30
3.2.2 Sample Recovery	32
3.2.3 Sample Analysis.....	32
3.2.4 Surface Area Measurements	34
3.3 Results.....	34
3.3.1 Preliminary Experiments	34
3.3.2 Effect of Milling Time and Media.....	34
3.3.3 Effect of Temperature	36
3.3.4 Milling with MoO ₃ and Silica.....	37
3.3.5 Surface Area Measurements	40
3.4 Discussion.....	41
3.5 Conclusions.....	44

CHAPTER 4: PRELIMINARY WORK ON NITRATION OF DIFFERENT ORGANIC COMPOUNDS	45
CHAPTER 5: CONCLUDING REMARKS	46
APPENDIX A: DERIVATION OF THE MILLING DOSE FORMULA	47
REFERENCES	49

CHAPTER 1: LITERATURE REVIEW

1.1 Introduction: Nitration Reactions

Some of the most common and important organic reactions involve nitration of various organic compounds [1]. Nitrated organic compounds find wide use in many applications. Majority of energetic materials, for example, are organic compounds, which derive their energy from the nitro group serving as an intramolecular oxidizer [2]. Nitrated aromatics are of particular interest as they are widely used as solvents, dyes [3], explosives [4], pharmaceuticals [5], and perfumes [6]. In addition, they serve as intermediates in preparation of other compounds, particularly amines [6]. Nitrotoluene (NT), for example, is the first precursor in the synthesis of trinitrotoluene – a common explosive [7, 8]. In addition, NT is used in synthesis of toluidine, nitrobenzaldehyde, and chloronitrotoluenes, which are the intermediates for the production of dyes, resin modifiers, optical brighteners and suntan lotions [9]. Other nitrated compounds, such as nitrocellulose and nitroglycerine also have a number of applications in energetic formulations (propellants, explosives, pyrotechnics) [10] and in pharmaceuticals [11]. The nitrating agent for these reactions has traditionally been fuming nitric acid combined with another strong acid, e.g., sulfuric acid, perchloric acid, selenic acid, hydrofluoric acid, boron trifluoride, or an ion-exchange resin containing sulfonic acid groups. These strong acids are catalysts that result in formation of nitronium ion, NO_2^+ . Sulfuric acid is almost always used industrially since it is both effective and relatively inexpensive [12, 13].

1.2 Shortcomings of Common Nitration Methods

The common nitration method described above has a number of disadvantages; perhaps the most significant being the production of large quantities of spent acid which has to be regenerated because its neutralization and disposal on a large scale is environmentally and economically unsound [14]. Another one is generation of considerable amounts of environmentally harmful waste during the purification of the products [15]. Other disadvantages include the hazards associated with handling the nitrating agent, as well as overnitration [16]. Furthermore, this reaction is not selective, and usually results in a mixture of isomers some of which are less desirable than others. For example, toluene nitration using this method produces a mixture of 55-60% of ortho- or o-NT, 35-40% of para- or p-NT, and 3-4% of meta-, or m-NT [12]. This leads to large quantities of unwanted product because the demand for p-NT is greater than for the other isomers [12, 17]. The conventional techniques used to increase the ratio of p- to o- isomers, such as nitration in the presence of phosphoric acid or in the presence of aromatic sulfonic acids increase the p/o ratio from 0.6 to 1.1-1.5 [12], but require additional use of environmentally harmful reactants. Another challenge associated with this reaction is the formation of oxidative byproducts. The addition of the nitro group to the aromatic ring of toluene strongly activates its methyl group making it susceptible to oxidation. Therefore, industrial nitration of toluene must be carried out at low temperatures to minimize

formation of the undesired oxidation products [12]. In a batch process, for example, the acids are added at 25°C and the reaction is carried out at 35 – 40°C[12]. The total NT yield in this reaction is 96% for a batch process, but most patents for continuous processes report yields of up to 50% [12].

1.3 Improved Nitration Methods

The disadvantages of the conventional approach to nitration have motivated research aimed at finding cleaner, safer, and more efficient methods. One direction of this research has been to replace liquid sulfuric acid with solid catalysts, which tend to be safer, environmentally friendlier, and easier to separate from the reaction solution than sulfuric acid. In addition, in the case of toluene nitration, surface reaction tends to favor formation of the desirable p-isomer [18].

Vassena, et al., [14] nitrated toluene in vapor phase using fuming nitric acid over solid acid catalysts. Several catalysts were tested, including zeolites and non-zeolitic materials. These can be divided into three groups: zeolites (ZSM-5, ZSM-12, beta and mordenite), non-microporous solid acids – Nafion® and Deloxan® (a polysiloxane bearing alkylsulfonic acid groups of Degussa), and preshaped silicas impregnated with sulfuric acid. The reactions were carried out in a fixed bed reactor at atmospheric pressure and at temperatures ranging from 130 °C to 160 °C.

The results of their experiments are shown in Figures 1.1-1.4. As seen from Figure 1.1, NT yield fluctuated around 20% for the reaction carried out without solid acid catalyst and around 40% for Deloxan catalyzed reaction. In both cases, the yield did not increase when the residence time was increased from 4 to 26 hours. Para/ortho ratio was approximately 0.7 for the uncatalyzed reaction and 0.8 for the reaction catalyzed with Deloxan®.

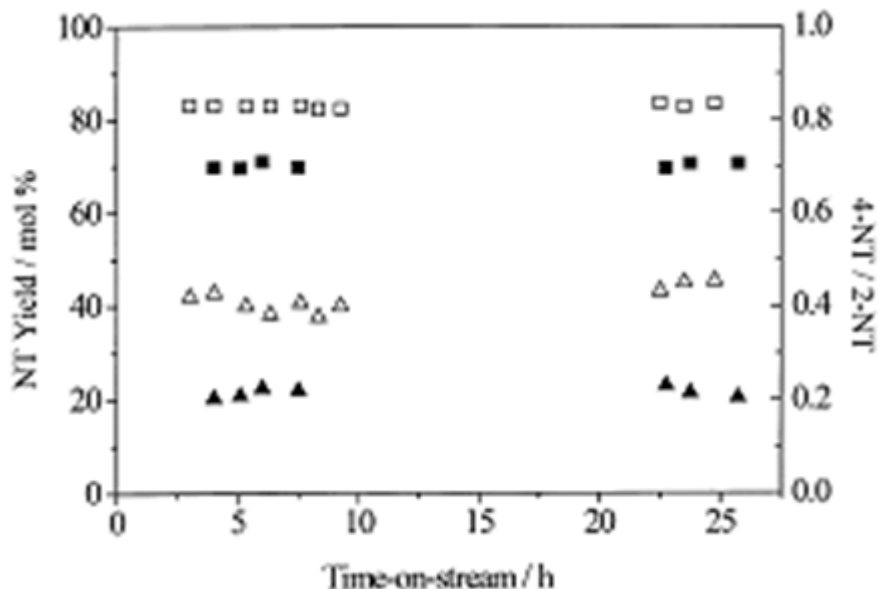


Figure 1.1 Vapor phase nitration of toluene: blank experiment and nitration with Deloxan. NT yield (left scale):(solid triangles)- without solid acid; (empty triangles) with Deloxan®. P/O ratio (right scale); (solid squares) – without solid acid, (empty squares) with Deloxan® [14].

Zeolite catalyzed reaction results are shown in Figure 1.2. As can be seen from the plot, NT yields for the zeolite-catalyzed reaction stayed close to 20%, but the p/o ratio varied from about 0.7 to about 1.1. This indicates that only some zeolites (namely H-beta) actually catalyzed the reaction, causing it to take place on the surface and thus resulting in a higher p/o ratio. Others did not affect the reaction, hence the yield stayed at 20%, same as for the uncatalyzed reaction, and the p/o ratio did not exceed 0.7, indicating a bulk reaction.

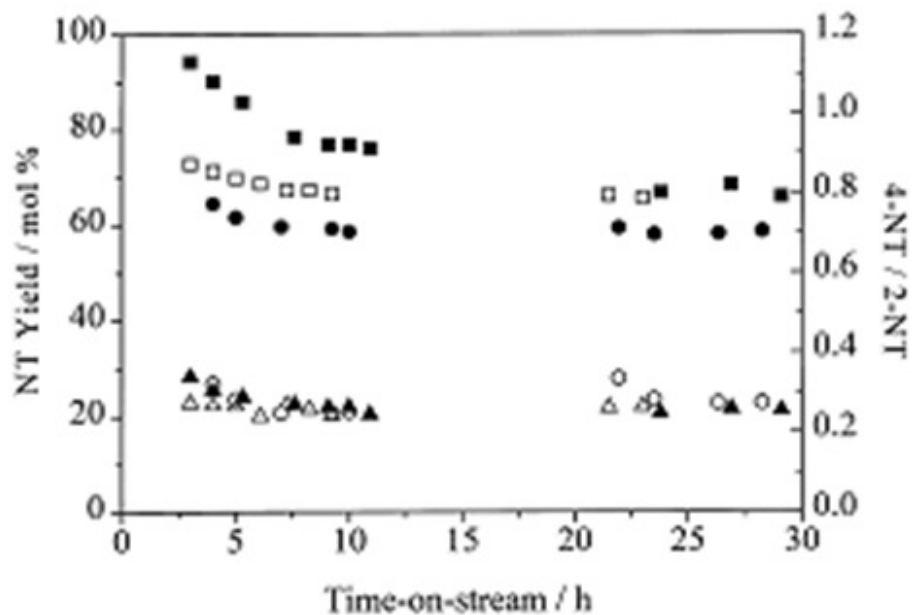


Figure 1.2 Vapor phase nitration of toluene with H-beta, H-ZSM-12 and H-ZSM-5. NT yield (left scale): solid triangle-H-beta; empty triangle - H-ZSM-5; empty circle - H-ZSM-12; P/O ratio (right scale): solid square -H-beta; empty square - H-ZSM-5; solid circle - H-ZSM-12 [14].

Figures 1.3 and 1.4 illustrate the results of toluene nitration over preshaped silica pellets impregnated with H₂SO₄ and over mordenite. The former was the only catalyst among those considered that produced NT yields of up to 60%, and even that only when the samples with high content of sulfuric acid were used.

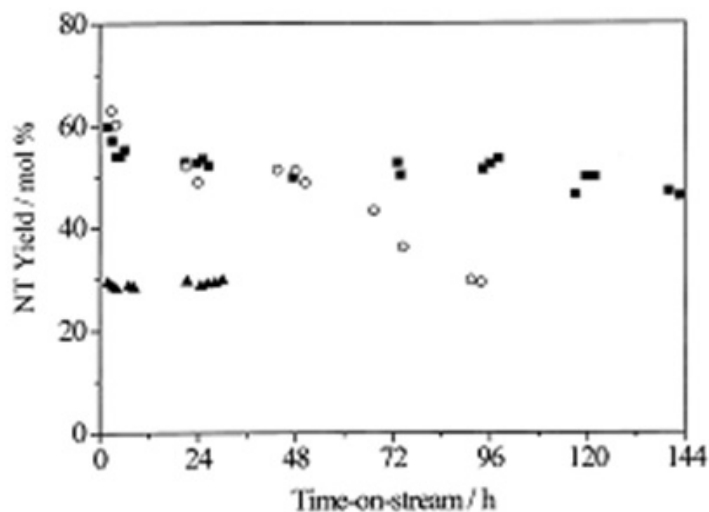


Figure 1.3 Results of a long-term experiment over preshaped silica impregnated with H₂SO₄. NT yield: solid squares - 80% H₂SO₄; open circles- 70% H₂SO₄; solid triangles - 8% H₂SO [14].

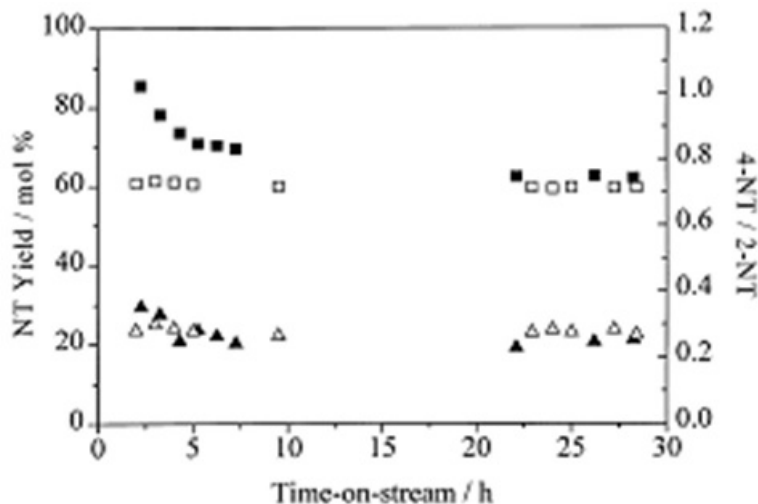


Figure 1.4 Vapor phase nitration over mordenite. NT yield (left scale): solid triangles- H-mor(74); open triangles- H-mor(4.6); P/O ratio (right scale): solid squares- H-mor(74); open squares- H-mor(4.6) [14].

The conclusion that can be drawn from their study is that among the catalysts considered, only silica impregnated with large loadings of H_2SO_4 produced reasonable product yields. Furthermore, while this catalyst does improve p/o isomer ratio, thereby addressing the problem of accumulation of unwanted products, it still requires use of fuming nitric acid as well as significant quantities of concentrated sulfuric acid. The latter, despite being attached to silica, gets used up and cannot be regenerated, as reported in the study. Therefore that approach does little to alleviate the environmental and the safety concerns associated with the traditional nitration methods.

In another study [19], the same group carried out a liquid phase nitration of toluene using 65% nitric acid over sulfuric acid impregnated silica and H-mordenite obtaining mono- and di- nitrotoluenes. High yields for both mono and di nitration were obtained with silica-supported sulfuric acid but the p/o ratio stayed at about 0.7. In addition, water produced as a byproduct had a negative effect on the yield. The reaction conditions and the results are listed in Table 1.1.

Table 1.1. Conditions and result of the liquid phase nitration of toluene [19]

Nitration of toluene using 50% H_2SO_4/SiO_2^a						
Cat H^+/HNO_3	Temperature ($^{\circ}C$)	Conversion (%)	NT Yield (%)	4-NT/2-NT	DNT Yield (%)	2,4-DNT/2,6-DNT
3.2	25	100	99.0	0.69	1.0	–
3.2	50	100	96.7	0.70	3.3	3.1
9.5	25	100	0.0	–	100.0	4.0
9.5 ^b	25	100	0.0	–	100.0	3.2

^a Reaction conditions: 3.2–3.8 g catalyst activated in static air at $120^{\circ}C$ for 18 h, 65 wt.% HNO_3 , HNO_3 /toluene = 2, solvent 10 ml CCl_4 , 24 h reaction time.

^b Regenerated and reused.

More recently Gong et al., [20], carried out liquid phase nitration of toluene using dilute nitric acid (50%) over silica supported Cs salt of phosphomolybdic acid

($\text{Cs}_{2.5}\text{H}_{0.5}\text{PMoO}_{40}$) and achieved remarkably high yields of up to 99.6% NT. The reaction was carried out in a stirred batch reactor with the highest product yields achieved at the reaction times of over 4 hrs. It was also found that the catalyst could be easily regenerated and reused. After separation by filtration, washing with distilled water several times and drying at 110 °C, it was reused several times and exhibited almost no drop in catalytic activity. The reaction conditions are summarized in Table 1.2 and the results are shown in Figure 1.5.

Table 1.2 Reaction Conditions For Toluene Nitration Over $\text{Cs}_{2.5}\text{H}_{0.5}\text{PMoO}_{40}$ Experiments [20].

Catalyst	BET surface area (m^2/g)	Pore Volume (cc/g)	E_i (mV) potentiometric titration	Toluene conversion ^a (%)	Selectivity (%)	
					ONT	PNT
CsPMA-5/ SiO_2	779	0.73	161	77.9	58.8	38.3
CsPMA-10/ SiO_2	598	0.69	358	95.4	58.7	38.2
CsPMA-20/ SiO_2	526	0.60	375	99.6	58.1	38.6
CsPMA-30/ SiO_2	358	0.32	219	93.5	58.3	38.5

^a The reaction conditions are the ratio by volume of toluene: Nitric acid is 1:3, the catalyst weight is 0.3 g, and the reaction is carried out at 70 °C under stirring for 3 h.

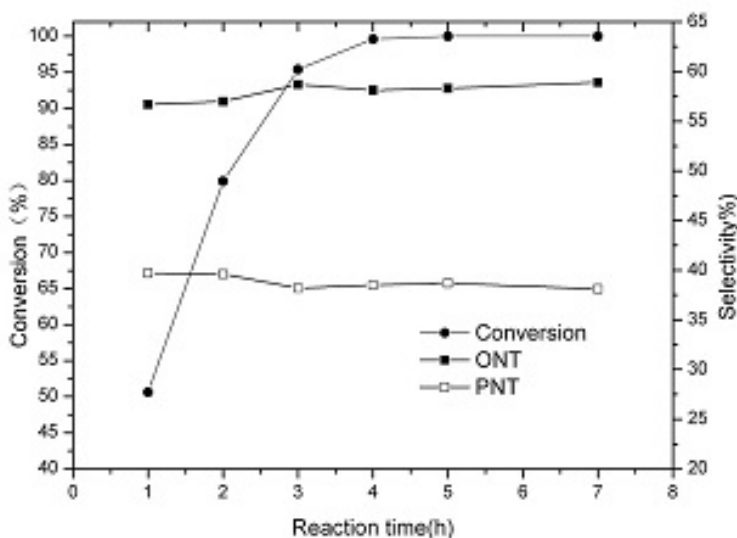


Figure 1.5 Effect of reaction time on the conversion of toluene over CsPMA-10/ SiO_2 [20].

This method has clear advantages over the ones discussed previously. It succeeded in eliminating the need for sulfuric acid, and even nitric acid was used in its dilute form offering clear benefits in terms of both safety and environmental impact. Furthermore, converting 99.6% of toluene to NT means that only a small amount of byproducts is generated, thus the need for purification is reduced. At the same time p/o isomer ratio for this method does not exceed 0.66, thus the problem of unwanted product accumulation persists.

In a similar vein, Adamiak et al., [21] achieved high yields of mono- and di- nitrotoluenes by nitrating toluene with fuming nitric acid over $\text{MoO}_3/\text{SiO}_2$ catalyst modified with H_3PO_4 . The characterization of catalyst showed that phosphoric acid reacted with

molybdenum oxide forming phosphomolybdic acid, which catalyzed the nitration reaction. Good para- selectivity was observed for this process with p/o ratios greater than 1 and reaching 2.09 in one case.

Table 1.3 Conditions and results of toluene nitration using H₃PO₄ modified MoO₃/SiO₂ catalyst [21].

Amount of H ₃ PO ₄ , wt.%	TN conversion, wt.%	Composition of product, wt.%		Composition of MNT, wt.%			Ratio p/o
		MNT	DNT	o-NT	m-NT	p-NT	
HPM	100	89.4	10.6	42.6	1.2	56.2	1.32
HPM ^a	10.5	88.5	11.5	31.6	2.8	65.6	2.09
6.4	100	98.6	1.4	47.1	1.0	51.9	1.10
5.7	100	92.8	7.2	43.0	1.3	55.7	1.30
5.7 ^a	74.1	94.6	5.3	44.0	0.7	55.3	1.26
5.7 ^b	33.5	88.5	11.5	47.1	1.3	51.6	1.10
1.4	100	85.0	15.0	42.4	0.9	56.7	1.34
0 [3]	92	100.0	-	48.0	1.7	50.3	1.05
Without catalyst	5.0	100	-	51.4	3.1	45.5	0.88

^a Second reaction using the same catalyst used in the first reaction.

^b The fifth reaction using the same catalyst as used in the previous reactions.

These approaches, however, still rely on nitric acid as the nitrating agent, which is a disadvantage in terms of safety and possible corrosion of the equipment. These concerns have prompted some researchers to consider other sources of nitronium ion. X. Peng et al., [22] carried out nitration of toluene using liquid NO₂ and molecular oxygen over zeolite catalysts and achieved p/o ratio as high as 14 using HZSM-5. Perves et al., [23] used nitronium tetrafluoroborate as a source of nitronium ion. These methods, however, while achieving promising results, rely on exotic and expensive reactants and/or catalysts. Therefore, they are not currently practical from the industrial standpoint.

1.4 Mechanochemically Induced Nitration Reactions

A new and potentially promising approach to this problem is to carry out the nitration reaction in solid phase using nitrate salts as sources of nitronium ion, with the reaction being driven by mechanical agitation, or mechanochemically. Eliminating solvents and acids offers substantial reduction of the environmental impact of nitration; using inexpensive and readily available nitrogen sources and catalysts offers potential cost benefits as well.

1.4.1 Mechanochemical Reactions

Although the concept of carrying out reactions in solid phase by mechanical agitation, known as mechanochemistry, has existed for centuries, with the earliest references to mechanochemical reactions dating back to 4th century BCE, its application has traditionally been limited to insoluble materials [24]. For soluble reactants, on the other hand, the default approach has been to carry out the reactions in solution [25]. Last several decades, however, have witnessed steadily increasing interest toward mechanochemical synthesis, and the manifestation of the versatility and the potential of this approach [26-38]. There are two reasons behind this recent boom in mechanochemical research. First, it is becoming increasingly clear that this approach can

be effective and even advantageous in a wide range of synthesis. Second, there is an increasing awareness that our current dependence on solvents is both wasteful of fossil derived materials, and harmful to the environment; thus it is unsustainable [25].

Table 1.4 lists some examples of reactions [25] that have been successfully carried out mechanochemically. This illustrates the versatility of the approach.

Table 1.4 Examples of Reactions That Have Been Carried out Mechanochemically.

Reaction	Comment
Metal halide reduction [39]	Performed by Michael Faraday in 1820
Alloying [40, 41]	One of the original applications, which is still important today. Metals or combinations of metal oxides with reducing agents can be used.
Cocrystallization [42]	Various types of cocrystals have been synthesized. Liquid assisted grinding often yields best results.
Knoevenagel condensation [43]	Important C-C bond forming reaction forming α - β unsaturated carbonyl compounds. First carried out mechanochemically in by Kaupp in 2003 [43]
Peptide synthesis [44]	Reducing the amount of solvents is one of the challenges of traditional peptide synthesis that is met by the mechanochemical approach [25].
Fullerene dimerization [45]	C ₁₂₀ dumbbell formed in high speed vibration milling
Synthesis of Molecular cages[46]	Very large covalent organic cages can be assembled by solvent-free ball milling[46]
Coordination polymerization (MOFs)	Ligand addition, ligand exchange, and acid base reactions involving coordination polymers have been carried out using various mechanochemical techniques such as liquid assisted grinding[47], and neat grinding[48]

A typical Knoevenagel condensation reaction carried out mechanochemically is illustrated in Figure 1.6. Use of stoichiometric amounts of reactants results in quantitative yield of the product. The temperature increase associated with ball milling plays an important role in promoting the reaction [25].

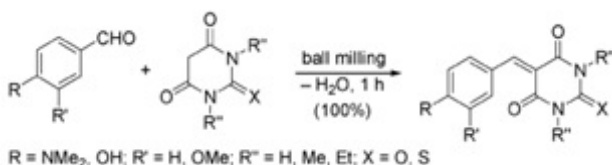


Figure 1.6 Knoevenagel condensation [25].

Figure 1.7 shows an example of an amidation reaction. Traditional methods for introduction of the amide group often require expensive transition metal catalysts and/or

toxic reactants. This solvent free route for direct amidation of aryl aldehydes with anilines in ball mill overcomes these problems[25].

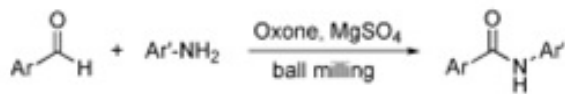


Figure 1.7 Direct oxidative amidation [25].

The solvent free peptide synthesis illustrated in Figure 1.8 results in high product yields using simple baking soda as a catalyst [25].

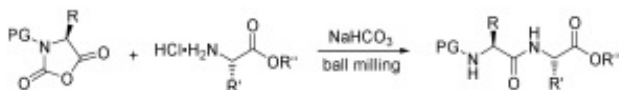


Figure 1.8 Solvent-free peptide synthesis [25].

Fullerene dimerization catalyzed by KCN (Figure 1.9) has been carried out by several research groups. Other potassium salts, such as carbonate and acetate also promote the reaction resulting in a mixture of the dimer and the unchanged C₆₀ in the ratio of 3:7 [45].

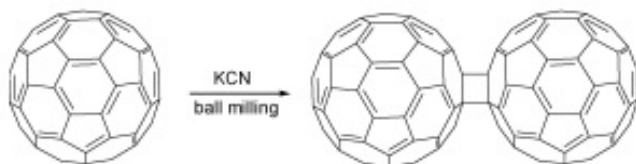


Figure 1.9 Fullerene dimerization [45].

Içli et al. [46] synthesized the molecular cage shown in Figure 1.10 in a ball mill with 71% yield. A smaller version of this cage was obtained in 94% yield compared to 24% yield obtained in solution. This reaction involves formation of 18 boronate ester and imine linkages between 11 components.

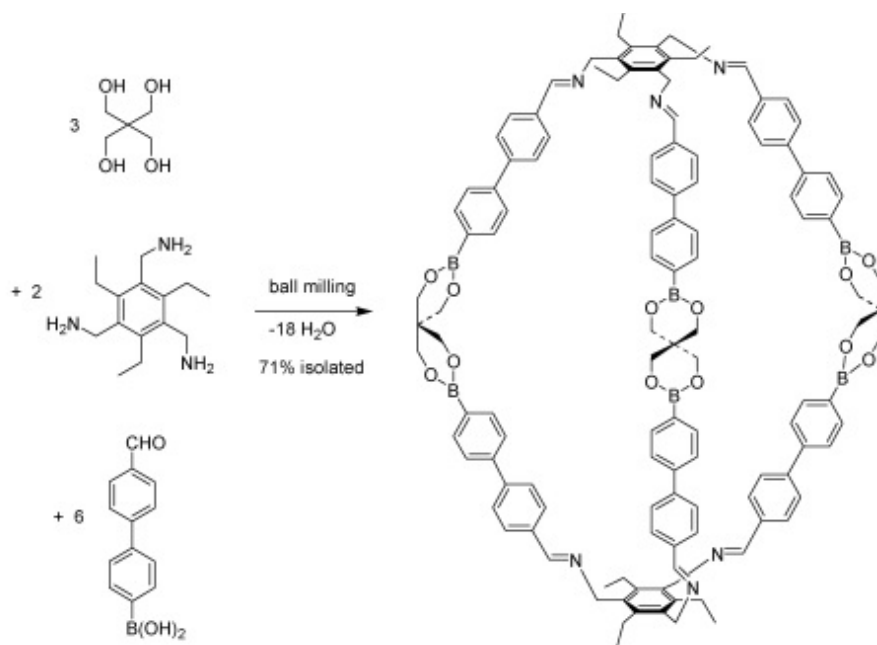


Figure 1.10 Solvent-free ball milling synthesis of a large organic cage [46].

Current understanding of the mechanisms of mechanochemical reactions is still rather deficient. A number of models have been proposed but their application in specific reactions is unclear. It is generally understood that the reactions occur at points of contact between solid surfaces rather than in the bulk of the material, but there are various theories explaining what occurs on these interfaces that causes the reactions to proceed. One possibility is that mechanical impact causes dramatic increase in lattice stress. This stress then relaxes, either physically, by emission of heat, or chemically, by ejection of atoms or electrons, formation of excited states on the surface, bond breakage, and other chemical transformations [49]. This can cause chemical reactions to occur in the field of mechanical stress or even after the stress is removed, by the action of reactive species such as free radicals formed under the action of mechanical stress, that can now cause the reaction to propagate further [49]. Other models discussed in the literature include the “hot-spot” theory and the “magma-plasma model” [50]. According to the former theory, small protuberances on the two surfaces sliding against each other cause plastic deformations associated with dramatic temperature increases. In the brittle materials, such increases can occur at the tips of propagating cracks. It is proposed that local temperatures in such hot spots can reach hundreds or thousands of degrees Celsius for very brief periods. According to the latter model, temperatures of the order of 10^4 °C can be generated at impact points. These can cause transient plasmas, and ejection of energetic species including free electrons [25]. It is not likely, however, that such high temperatures occur to a significant extent in organic reactions because if they did, they would cause decomposition of many species [25]. Instead, covalent bond forming organic reactions have been suggested to occur through the formation of intermediate liquid eutectic phases [25]. There has been little study on the application of these mechanisms to specific reactions, despite the fact that the parameters affecting the process can depend significantly on the specific mechanism. Lowering temperature, for

example, usually improves the effectiveness of milling processes, and can improve the rate of reactions caused by formation of surface defects. If, however, the reaction proceeds through the formation of a localized liquid phase, its rate is likely to drop when the temperature is lowered.

1.4.2 Mechanochemical Nitration of Organic Compounds

Despite the wide variety of reactions that have been carried out mechanochemically to date, nitration of aromatics has been largely overlooked. An exception is the work of J. Albadi et al., [6] who nitrated a number of aromatic compounds in a mortar using sodium nitrate in the presence of melamine trisulfonic acid (MTSA) as a source of nitronium ion. The reaction times ranged from 5 to 60 minutes and the nitrated products were obtained with high yields. Table 1.5 lists the aromatic compounds successfully nitrated in their study.

Table 1.5 List of aromatic compounds nitrated by J. Albadi, et al., [6].

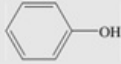
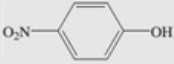
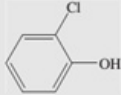
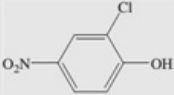

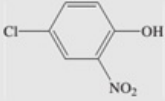
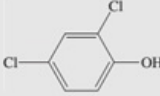
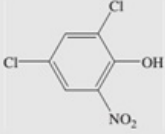
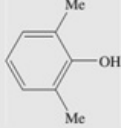
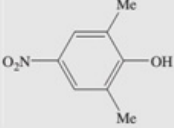
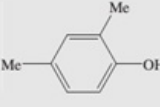
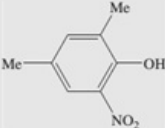
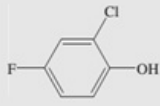
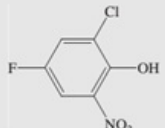
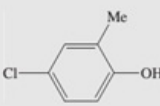
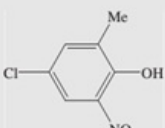
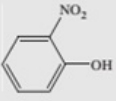
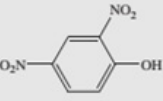
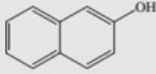
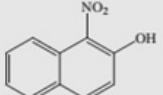
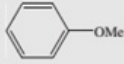

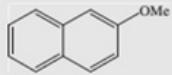
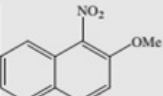

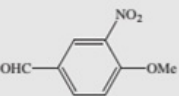
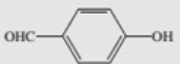
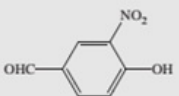
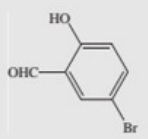
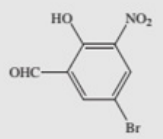
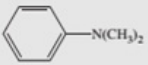
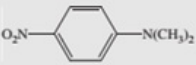
Entry	Substrate	Product	Time (min)	Yield (%) ^a
1			5	87
2			12	88
3			30	86
4			55	87
5			5	89
6			30	87
7			22	89
8			18	87

Table 1.5 continued

Entry	Substrate	Product	Time (min)	Yield (%) ^a
9			30	88
10			60	82
11			15	88
12			60	75
13			45	82
14			32	85
15			30	87
16			5	86

^a Isolated yield.

It is worth pointing out, however, that all the compounds nitrated in that study were activated by strongly electron donating substituents such as the $-\text{OH}$, $-\text{OMe}$, or $-\text{N}(\text{CH}_3)_2$ groups. Nitration of toluene, whose methyl group is less activating in an electrophilic substitution reaction than the above listed groups, was not reported in that article.

In this study, we take the approach of mechanochemical nitration using nitrates a step further by using environmentally benign catalysts, such as MoO_3 or combinations of MoO_3 and SiO_2 to nitrate toluene in a ball mill. Unlike MTSA, unmilled MoO_3 is not an acid, but under the vigorous mechanical impacts of the ball milling process, it has been found (see Chapter 2) to acquire acidic properties allowing it to catalyze the formation of nitronium ion from sodium nitrate.

The catalytic activity of MoO_3 , particularly in hydrocarbon oxidation reactions has long been known, and many studies have been performed examining its use in partial oxidation of methanol [51, 52] and other compounds [51]. Although the mechanism of

these reactions is subject to much debate in the literature [51], there is evidence, based on atomic force microscopy studies performed by Smith and Rohrer [53], that the uncoordinated Mo^{6+} cations on step edges and defects are the active sites for oxidation of alcohols. These electrophilic cations also possess Lewis acid properties, and therefore can catalyze formation of the nitronium ion from the nitrate. Thus the ball milling process, which breaks the crystals forming many new defects can be used to greatly enhance the Lewis acid properties of MoO_3 making it an effective catalyst in mechanochemical aromatic nitration reactions.

CHAPTER 2: MECHANOCHEMICAL NITRATION OF TOLUENE: FEASIBILITY¹

2.1 Introduction

Nitration of aromatic compounds is a common reaction used for preparation of multiple organic energetic materials, including TNT, NTO, and others[54-56]. The reaction is an electrophilic aromatic substitution; its practical implementations typically involve multiple liquid reagents. An important case is the nitration of toluene with mixed acids: nitric acid/sulfuric acid, nitric acid/aromatic sulfonic acid or nitric acid/phosphoric acid[57]. While the technology is well established, it is associated with a number of environmental and safety concerns[58]. Most significantly, it generates red water from the sulfiting process for removing unsymmetrical trinitrotoluene isomers [15]. Such concerns stimulate active research on remediation of the red water and other waste generated by nitration of organic compounds on the industrial scale, e.g., see most recent papers [59-62]. New safe and environmentally friendly manufacturing approaches are being actively explored[63, 64]. In one example, recently implemented in a commercial process, an environmentally friendlier method of manufacturing TNT was developed at Radford Army Ammunition Plant operated by ATK [65]. The process involves replacing toluene as a starting material with ortho-mononitrotoluene. Using a nitro compound as a precursor streamlines the following operation; however, ortho-mononitrotoluene needs to be prepared elsewhere, and the associated environmental waste-related issues are being locally bypassed rather than completely solved.

Recently, ideas of mechanochemical synthesis originally developed for metal-based materials and inorganic composites have been extended to include synthesis and modification of various organic compounds [25, 66-69]. Although this technology consumes substantial energy, it is readily scalable. It also offers the possibility to eliminate solvents from the process, which has been a significant incentive for its exploration. It is currently considered for preparation of a broad range of organic and inorganic materials, composites, and structures. This work explores the feasibility of mechanochemical processing for nitration of aromatic compounds. If successful, this

¹ Journal Article published in Journal of Energetic Materials, July 2017

technology can be developed into an environmentally friendly, solvent free manufacturing method for a wide range of energetic materials or their precursors.

The nitrate source in this study is sodium nitrate, a readily available, environmentally benign solid. The concept of using sodium nitrate in the presence of an acid as a nitrating agent is not new. However, much more aggressive Lewis acids, e.g., AlCl_3 , are used commonly. Working with such materials and disposing of the related chlorinated byproducts is still undesirable. Qian, et al, performed nitration of phenols in solvent free conditions using metal nitrates in the presence of oxalic acid as the nitrating agent[70]. Oxalic acid, too, however, is a relatively strong acid; in addition, his work was only with phenols, which are strongly activated towards electrophilic aromatic substitution. Therefore, in this work, molybdenum trioxide, MoO_3 , which has Lewis acid surface sites, was explored as potential catalyst for nitration. This oxide has long been known for its catalytic properties in a number of reactions including nitration of aromatic compounds. Skupinski, et. al, for example, used $\text{MoO}_3/\text{SiO}_2$ to obtain high yields of mononitrotoluene by nitration of toluene with 65% nitric acid[71]. Kemdeo, et al, studied the use of $\text{MoO}_3/(\text{TiO}_2/\text{SiO}_2)$ in nitration of phenol[72], and $\text{MoO}_3/(\text{SiO}_2\text{-ZrO}_2)$ in nitration of toluene[73]. Adamiak, et al, explored the mechanism of toluene nitration over $\text{MoO}_3\text{-SiO}_2$ [74], and in another study enhanced this catalyst by addition of H_3PO_4 with excellent results[21]. In all of these studies, however, MoO_3 was used in combination with other metal oxides, and its function was to enhance the acidity of the Bronsted sites present on the surface of silica, titania or zirconia. In the last case it reacted with phosphoric acid to form phosphomolibdic acid – one of the strongest inorganic acids known. These Bronstead acids protonated HNO_3 , leading to formation of nitronium ions, instead of H_2SO_4 normally used for this purpose. In this study, on the other hand, MoO_3 was used without any support and the source of nitronium ion was NaNO_3 rather than nitric acid – a much more environmentally friendly and easy to handle alternative. These solid reactants, sodium nitrate, NaNO_3 , as a source of the nitro-group and molybdenum trioxide, MoO_3 , as a Lewis acid catalyst, were ball-milled with toluene in order to produce the reaction:



The objective is to demonstrate the feasibility of mechanochemical nitration of toluene using environmentally benign reagents, and to explore how process parameters affect product yield and selectivity.

2.2 Experimental

Nitration of toluene was achieved using mechanical milling of toluene, sodium nitrate, and molybdenum oxide as a catalyst. Materials used in the experiments were toluene (Chempure, 99.99 %), molybdenum oxide, MoO_3 (Alfa-Aesar, 99.95 %), and sodium nitrate (Alfa Aesar, 99%). Ethyl acetate (Alfa Aesar, 99.5 %) was used to extract the

reaction products for analysis. Two ball mills were used. A Spex Certiprep 8000D shaker mill (SM) was used for samples of up to 6 g, and a Retsch PM 400MA planetary mill (PM) was used for larger samples of up to 50 g. In both cases, hardened steel vials were used and 9.5 mm (3/8") hardened steel balls served as milling media. Steel balls with 3.2 mm (1/8") diameter were used in one experiment.

Preliminary experiments established the feasibility of mechanochemical formation of ortho- and para-mononitrotoluene, although at low yields. All subsequent experiments were performed in an effort to determine parameters affecting the mononitrotoluene yield and selectivity. The parameters varied were the ball-to-powder mass ratio (BPR) and the relative proportions of the starting reagents.

Table 2.1 summarizes these milling conditions for a set of runs with milling duration of 2 hours. Longer milling times were used in several runs, which are discussed separately. Table 2.1 also shows symbols used to represent the results of different milling runs in subsequent figures. A visual representation of the various charge compositions is given in Fig. 2.1 in the form of a ternary compositional diagram.

For most runs, the mole fraction of toluene is relatively low, varying from 6.3 to 4.4 %, as represented by points lined along the MoO_3 - NaNO_3 axis. The $\text{MoO}_3/\text{NaNO}_3$ ratio varies in a broad range, and several points are available with substantially varied toluene/solid ratios. Along with Table 2.1, Fig. 2.1 should be used to interpret the experimental results discussed below. Note that some of the points, e.g., filled and open stars, overlap in Fig. 2.1.

The milling runs are divided into several groups. In the largest group, milled in the shaker mill and represented by open squares, the relative amounts of NaNO_3 and MoO_3 were varied, the amount of toluene was fixed at 0.25 mL, and the total mass of solids was fixed at 5 g. The crossed open circle represents an experiment from the same set, with the MoO_3 to NaNO_3 molar ratio of 2.95, identical to one of the hollow squares, except in this case toluene was added after 95 minutes, 25 min before the end of the milling process.

Open and filled triangles represent two experiments in which the amounts of all reactants were doubled (10g of solids and 0.50 ml of toluene) thereby lowering the BPR to 5. The mole ratios of MoO_3 to NaNO_3 were 2.94 (filled triangle) and 3.54 (open triangle).

Filled circles and diamonds represent experiments examining the effect of increasing amounts of toluene. The MoO_3 to NaNO_3 mole ratio is 1.47 for the circle, and 5.96 for the diamond. In both cases, the toluene amount was increased to 1 ml while maintaining the total mass of solids at 5 g.

The half-filled circles represent runs in which the amount of NaNO_3 was increased without changing the amounts of MoO_3 (4.17 g, as in the experiment represented by an open, crossed circle) and toluene (0.25 ml), thus raising the total mass of solids. The mass of NaNO_3 was doubled from 0.83 to 1.66 g.

The asterisk represents an early experiment with a much higher toluene/solids mass ratio. It used 1.1 ml of toluene and a total of 1.7 g of solids.

The stars represent two planetary mill runs with different milling ball sizes. In these runs, the toluene/solid ratio could be reduced further, while using a well-defined 0.5-ml volume of toluene.

Table 2.1 Summary of the Milling Conditions for 2-hr Runs

Symbol	Mill	Ball diam., mm	BPR	Solid mass, g	Molar ratios			Mass ratio
					MoO ₃ /NaNO ₃	MoO ₃ /toluene	NaNO ₃ /toluene	Toluene/solid
□, ⊗*	SM	9.5	10	5	0.296-28.92	4.91-14.39	0.995-16.57	0.043
▲	SM	9.5	5	10	2.94	12.2	4.15	0.043
△	SM	9.5	5	10	3.54	12.6	3.55	0.043
●	SM	9.5	10	5	1.47	2.62	1.78	0.174
◐	SM	9.5	8.6	5.85	1.48	12.24	8.29	0.037
◆	SM	9.5	10	5	5.96	3.34	0.559	0.174
⊗	SM	9.5	10	1.76	0.98	0.708	0.72	0.564
☆	PM	9.5	3	43.3	14.75	61.2	4.15	0.010
★	PM	3.2	3	43.3	14.75	61.2	4.15	0.010

*toluene was added 25 minutes before the end of the run.

In addition to the experiments summarized in Table 1, a limited number of experiments were conducted at longer milling times. Specifically, charge compositions with MoO₃/NaNO₃ ratios of 2.95 and 1.47, milled with 0.25 mL of toluene were milled for 4, 6, and 8 hours.

After milling, the materials were extracted with ethyl acetate, separated from the solid inorganic fraction *by settling* and analyzed in a HP 6890 gas chromatographer (heating profile: 40 °C to 300 °C at 5 K/min) coupled with HP G2350A mass spectrometer. Product species were identified using the NIST Mass Spectral Library (NIST 08), and relative concentrations were determined using GC peak integration. To quantify the results in terms of yield and selectivity, five major byproducts were selected: benzaldehyde, 2,2'-dimethyl-biphenyl, 1-methyl-4-phenylmethyl benzene, 2-methylphenyl-phenylmethanone, and 4-methylphenyl-phenylmethanone. The mononitrotoluene yield was estimated by evaluating the ratio of the sum of all peak areas of mononitrotoluene to the sum of the areas of peaks of toluene and of the above byproducts. The undesired byproduct yield was calculated similarly, and the selectivity was calculated as the ratio of mononitrotoluene yield to the byproduct yield. Effectively, it was the ratio of the areas of all mononitrotoluene peaks to the area of peaks of all the

byproducts. Peak areas for all mononitrotoluene isomers were combined for both yield and selectivity assessments.

The specific surface area of MoO₃ was measured before and after milling with NaNO₃ and toluene via *single*-point BET nitrogen adsorption, using a Horiba SA-9600 surface area analyzer. The specimens were outgassed in the instrument cell in a stream of dry N₂ at 150 °C for three hours prior to the measurement. The measurements were run in duplicates.

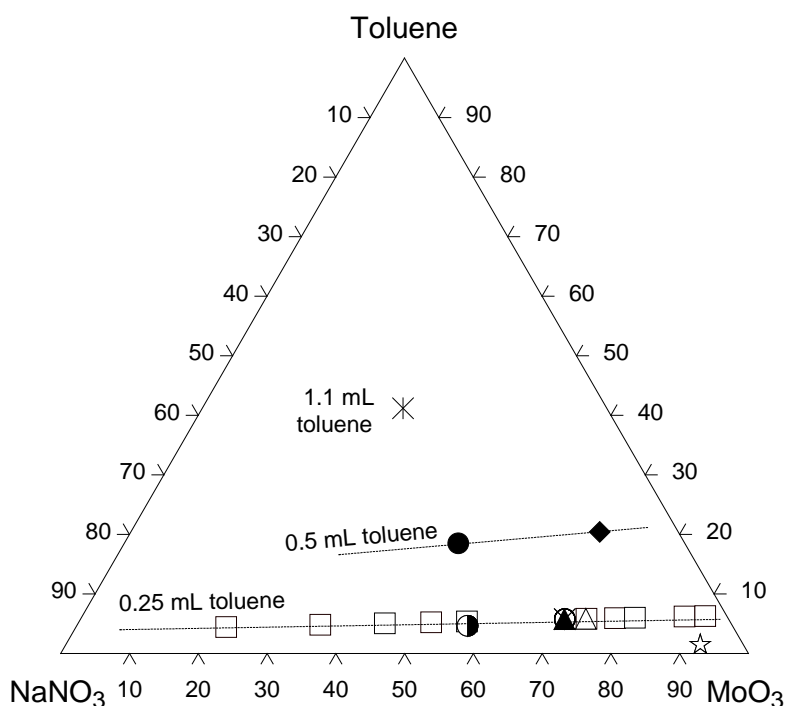


Figure 2.11 Ternary diagram showing relative amounts of the reactants in the 2 hr milling experiments.

2.3 Results

2.3.1 Formation of Mononitrotoluene with MoO₃ as a Catalyst

In preliminary, exploratory experiments, toluene and sodium nitrate were milled with several metal oxides with Lewis acid surface sites. These included WO₃, TiO₂, Al₂O₃ and ZrO₂. No nitration was observed, and therefore these materials were not further investigated.

Toluene was successfully nitrated by milling it with NaNO₃ and MoO₃. Characteristic GC-MS traces are shown in Fig. 2.2. The top and bottom traces represent 2-hr SM and PM runs, respectively. Each trace is labeled with the symbol representing the run in Table 1. For the SM run, the specific mole ratios of the reactants were: MoO₃/NaNO₃=3.6;

$\text{NaNO}_3/\text{Toluene}=3.53$. In Fig. 2.2, the peaks on the left of the toluene peaks represent ethyl acetate and are not labeled. In both cases, mononitrotoluene is present as a mixture of isomers. In addition, a number of undesired byproducts are also observed, such as toluene dimers, benzaldehyde, and benzoic acid among others.

The toluene peak on the bottom trace, corresponding to the PM experiment, is very narrow. Most of toluene was converted to either mononitrotoluene or the byproducts. Yield exceeding 40% of nitrotoluene was attained in this PM run with a relatively short milling time of 2 hours. In addition to a high yield, the selectivity of mononitrotoluene production also improved, with substantially greater ratio of the area of the mononitrotoluene peaks to those of other products (benzaldehyde, 1-methyl-4-phenylmethylbenzene, etc.) This clearly shows that the mechanochemical approach offers a feasible way of nitrating toluene with no harmful chemicals and byproducts.

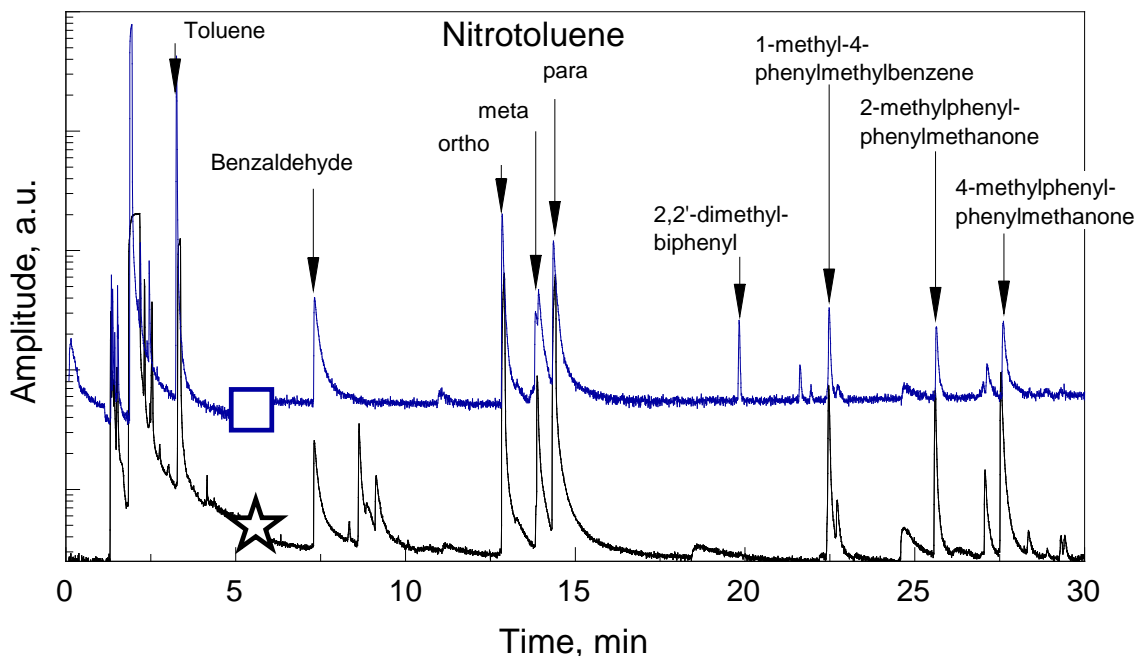


Figure 2.2 GCMS traces for selected mechanochemical experiments on nitration of toluene. Top: SM; bottom: PM. The mononitrotoluene yield and selectivity respectively are 18.2% and 2.7 for the top, and 42.2% and 4.97 for the bottom traces.

2.3.2 Parameters Affecting the Product Yield

Figures 2.3 – 2.5 show yield and selectivity of mononitrotoluene production as a function of molar ratios of different materials used in the milling runs. The symbols used in all figures are the same as those shown in Table 2.1. To simplify the interpretation of these results, only 2 hour milling runs are included in this set of plots. Data for both yield and selectivity appear to produce peaks in each of the shown plots.

In most cases, the yield and selectivity correlate with each other. All points with particularly low yields: asterisk, filled circle, and diamond, (except for one open square), correspond to relatively large amounts of toluene used; cf. Table 2.1 and Fig. 2.1; these points are shifted to the left in Fig. 2.5, because of the low MoO₃/toluene ratios. The only exception where a low yield is observed for a relatively small amount of toluene is an open square point (appearing in all Figs. 2.3 – 2.5) with the very low concentration of NaNO₃, for which the composition is shown at the left bottom corner in Fig. 2.1. Conversely, the experiments performed using the PM, for which the ratio of MoO₃ to toluene was particularly high (points are shifted to the right in Fig. 2.5), produced higher yields than the SM experiments with the same ratios of NaNO₃/MoO₃ and NaNO₃/toluene.

For the same toluene to solid mass ratio of 0.43, the data for both yield and selectivity form relatively clear peaks in both Figs. 2.3 and 2.4. In Fig. 2.3, the peak is relatively broad and is located at the range of NaNO₃/toluene ratios of 1 – 4. In Fig. 2.4, the peak corresponds to the MoO₃/NaNO₃ ratios of 3 – 15.

Data points in Fig. 2.5 form a highly asymmetric peak, with a sharply falling right edge. This peak structure can be understood considering that the same points, for which the toluene/MoO₃ ratio becomes large, have a much reduced amount of NaNO₃ (because the total mass of solid remains fixed at 5 g, see Table 2.1.) Thus, the effect is simply associated with the NaNO₃ deficiency, which is not explicitly seen from Fig. 2.5.

The yield for the run represented by a crossed circle, for which milling was initially dry and toluene was added later in the process coincides with that of the similar run, where toluene was loaded to the milling vial from the very beginning. However, the selectivity represented by the crossed circle run is lower, suggesting that more byproducts formed.

The yield for data points represented by half-filled circles fits well with the trend formed by open squares, suggesting that the increase in the concentration of NaNO₃ did not change the yield. The selectivity for the half-filled circles was reduced compared to that shown by the open squares.

The data points represented by triangles correspond to a reduced BPR and thus reduced milling dose, which is a measure of the specific energy transferred to the material from the milling tools. These data show a reduced yield compared to the runs represented by open squares and corresponding to a greater milling dose. In qualitative agreement with this observation, for PM runs, the yield is higher for the run represented by an open star, for which larger size balls were used. Although the BPR was the same for both PM runs, larger size balls result in greater impact energies transferred to the material being milled.

The data points characterizing yield appear to be slightly less scattered than the corresponding data on selectivity. This could simply indicate that the selectivity assessment was prone to more errors.

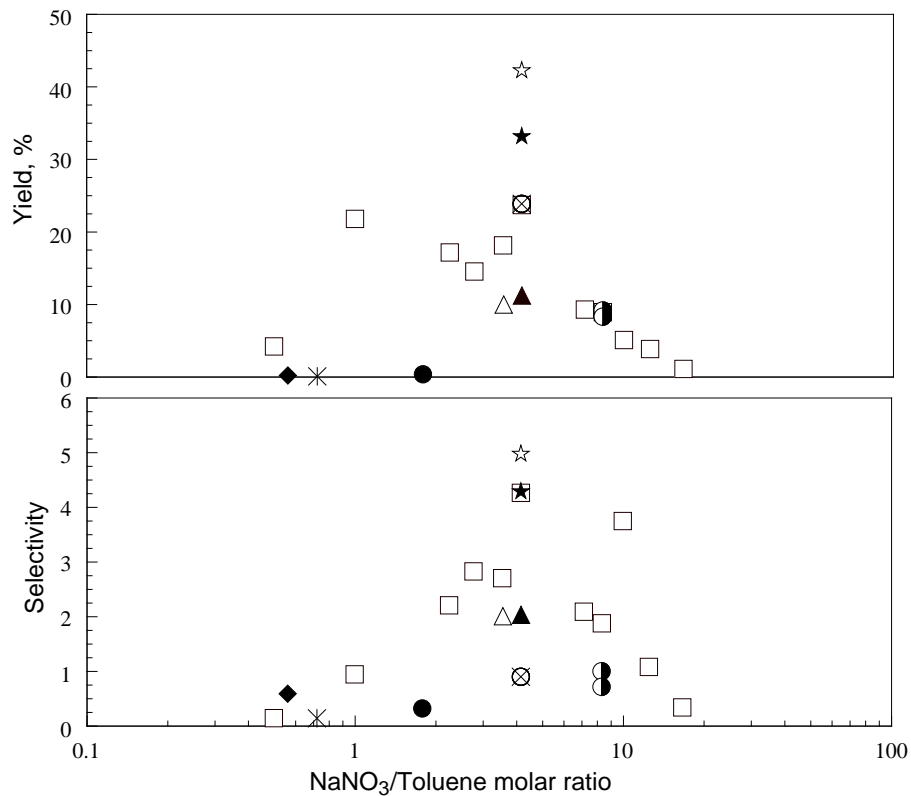


Figure 2.3 Mononitrotoluene yield and selectivity vs. NaNO_3 /toluene molar ratio. Milling time is 2 h.

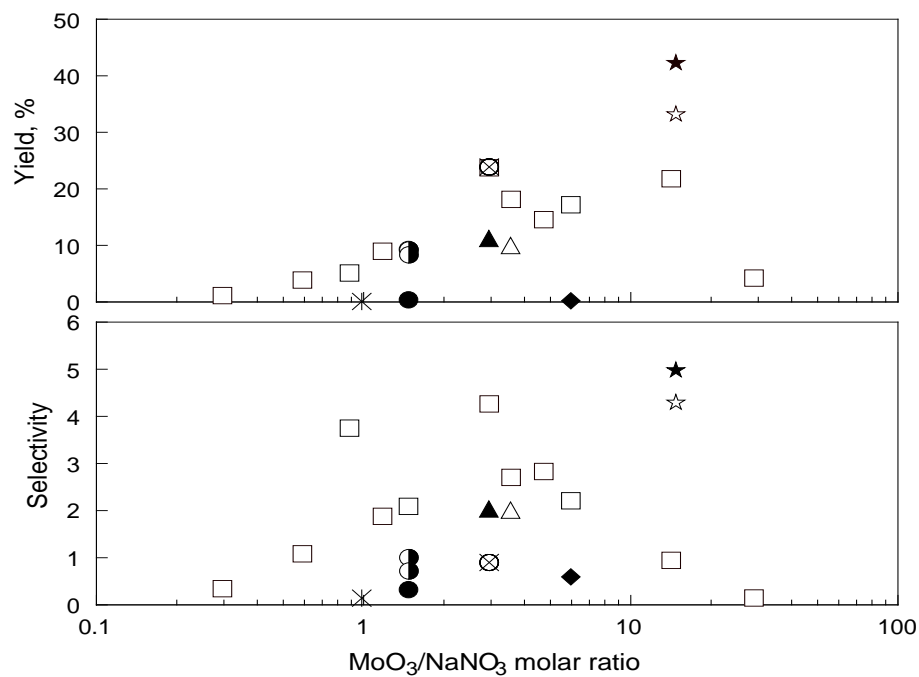


Figure 2.4 Mononitrotoluene yield and selectivity vs. $\text{MoO}_3/\text{NaNO}_3$ molar ratio. Milling time is 2 h.

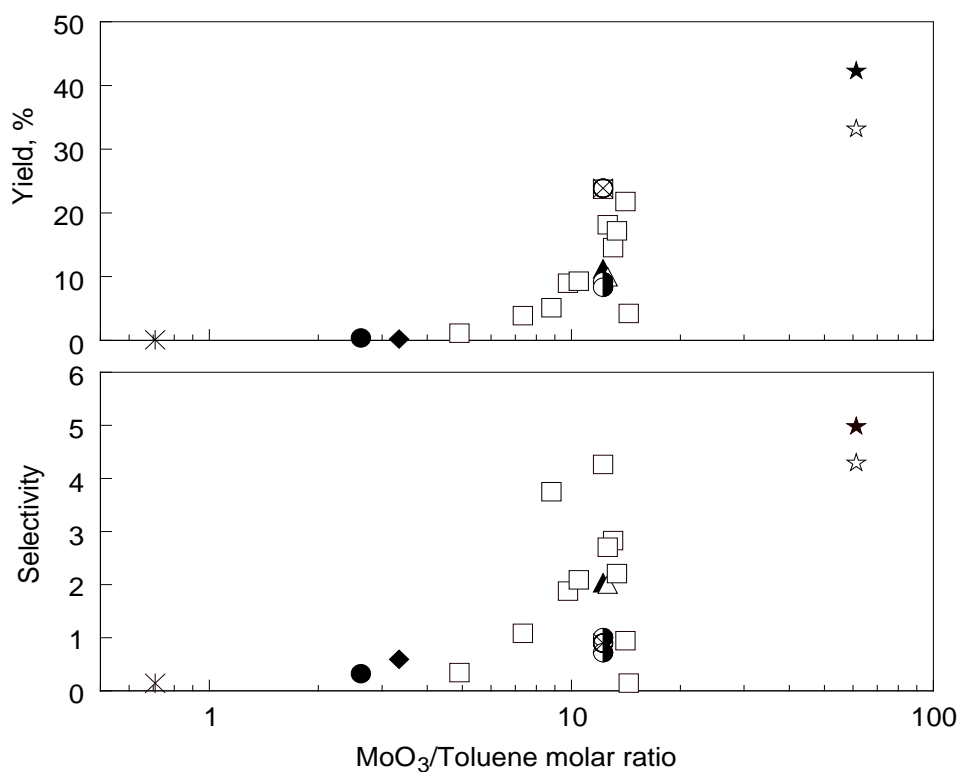


Figure 2.5 Mononitrotoluene yield and selectivity vs. MoO₃/toluene molar ratio. Milling time is 2 h.

A correlation between the yield and selectivity is well observed from Fig. 2.6, where these values are plotted against each other. This correlation is important, as suggesting that further optimization of the mechanochemical nitration of toluene is likely to generate a cleaner product.

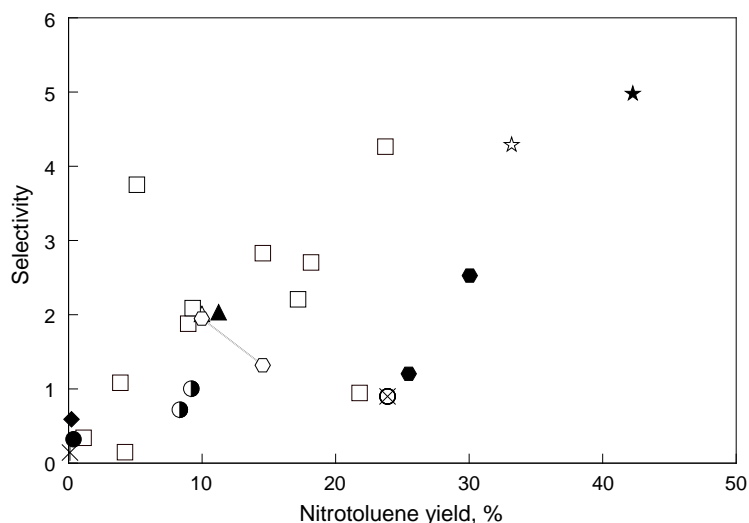


Figure 2.6 Selectivity vs. mononitrotoluene yield. Symbols for 2-h runs are as shown in Table 1. Filled and open hexagons show points, for which the milling dose was varied. Additional details are given in Figure 2.7.

The effect of milling dose on yield and selectivity of the toluene nitration is illustrated in Figure 2.7. For this simplified analysis, the milling dose was estimated as a product of BPR and milling time. Such an estimate can be used to compare runs with the same ball size and performed using the same mill [75-77]. The data in Figure 2.7 include two subsets of SM experiments with $\text{MoO}_3/\text{NaNO}_3$ ratios of 2.95 and 1.47. The variation of both milling times and BPR affected the milling dose. It is apparent that the increasing milling dose leads to a greater yield; although a saturation seems to occur, especially for the experiments with the $\text{MoO}_3/\text{NaNO}_3$ ratio of 2.95. It is also apparent that unlike results shown in Figs. 2.3 – 2.5, an increase in yield due to a greater milling dose may reduce selectivity, which is an undesirable effect. Additional experiments varying milling dose are needed, in particular, with lower amounts of toluene, observed to increase the mononitrotoluene yield, to observe the practical maximum achievable for both yield and selectivity.

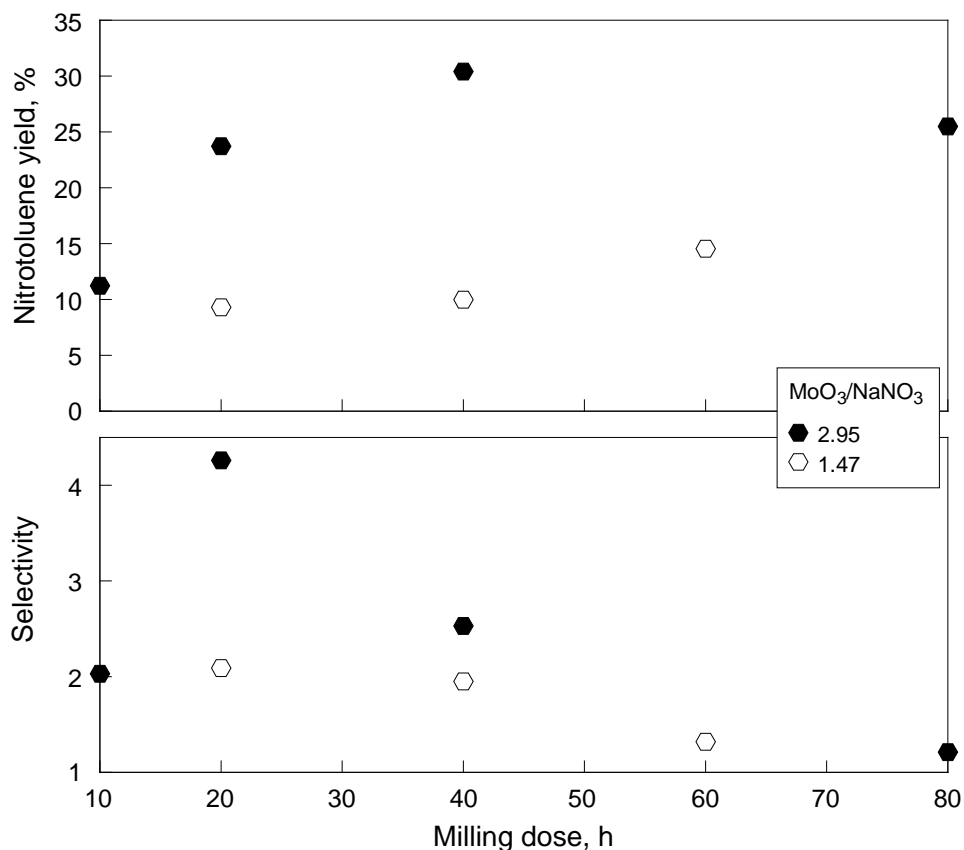


Figure 2.7 Mononitrotoluene yield and selectivity vs. milling dose. The point at milling dose of 10 h corresponds to a 2-h milling run with BPR 5, for other points, BPR was 10 and the milling time varied between 2 and 8 h.

To establish the development of the MoO₃ surface, the location of catalytic Lewis acid sites, as it is being milled, several MoO₃ samples were prepared using various milling conditions and their surface areas were measured using BET. All samples contained 4.167 g of MoO₃ loaded in a SM vial with 10-mm balls. The BPR was fixed at 10. The milling time was set to 2 hours. Amounts of toluene added in each experiment varied. Results are shown in Table 2.2. Milling increases surface area markedly, and milling in the presence of toluene increases the surface area more than milling without toluene. However, varying the amount of toluene does not seem to affect the surface area of MoO₃.

Table 2.2 Specific Surface Area For Unmilled And Milled MoO₃ Samples. Results Reflect Two Repeat Measurements

	Volume of toluene, ml	Surface area, m ² /g
initial MoO ₃	0	0.23 ± 0
MoO ₃ milled for 2 h with MoO ₃ /NaNO ₃ of 2.96	0	3.14 ± 0.07
	0.25	20.2 ± 0.5
	0.50	19.6 ± 0.1
	0.75	19.7 ± 0.8

2.4 Discussion

A higher yield of nitrated products is observed for the NaNO_3 /Toluene molar ratio in the range of 1 – 4 (Fig. 2.3). Of the experiments performed with 0.25 mL toluene in the shaker mill (open squares), the highest yield is observed near the stoichiometric NaNO_3 /toluene molar ratio of 1. Almost no yield is observed for higher amounts of toluene (filled circle, diamond, and asterisk), while the highest yield was observed for a much lower toluene/solids ratio in the planetary mill (open star). This suggests that the reaction is limited by the available catalytic surface sites, and providing excess toluene does not result in greater degree of nitration. This is further illustrated in Fig. 2.5 showing the observed yield vs. the MoO_3 /toluene ratio. This ratio did not affect the specific surface area of MoO_3 (cf. Table 2.2) suggesting that the number of active sites on the MoO_3 surface did not change. Instead, the change in yield as a function of the MoO_3 /toluene ratio was likely caused by the balanced interaction of toluene and NaNO_3 molecules adhered at the available surface active sites of MoO_3 . Assuming that the toluene/ NaNO_3 reaction occurred between components located at neighboring active sites on surface of MoO_3 , one expects that excess of toluene may lead to many active sites occupied by toluene with no nearby NaNO_3 . In this case, the yield is reduced, as observed experimentally for low MoO_3 /toluene ratios. The yield is also reduced, as expected, for very low NaNO_3 concentrations.

The number of active sites is expected to increase as a function of the milling time or milling dose, explaining an observed greater mononitrotoluene yield for an increased milling dose. It is suggested that an increased amount of MoO_3 should generally lead to a greater yield generating more active sites at which the reaction can occur.

It is less clear how the selectivity of toluene nitration was affected by the process parameters. A number of parameters, which were not carefully monitored, could have affected the selectivity, which justifies the need in an additional study. For example, the milling vial temperature, which is expected to vary as a function of the amount of toluene (serving also as a liquid process control agent and lubricant), the total solid load, BPR, and other parameters could have affected the selectivity substantially.

2.5 Conclusions

Feasibility of mechanochemical nitration of toluene is shown using NaNO_3 as a reactant and MoO_3 as a catalyst. This study is the first, to the authors' knowledge, to report nitration of toluene with molybdenum oxide - a safe to handle, relatively inert compound which has been reported to have weak Lewis acid properties. It does not catalyze the reaction between NaNO_3 and toluene in a test tube, but under mechanical impact it was found to catalyze aromatic nitration, with the yields increasing with the amount of milling. Several other metal oxides were also explored as potential Lewis acids, including WO_3 , TiO_2 , Al_2O_3 and ZrO_2 with negative results.

The yield exceeding 40% of mononitrotoluene has been attained, and a higher yield is expected to be possible with further optimization of the process parameters. An increase in yield is accompanied with a greater selectivity of preparation of mononitrotoluene, suggesting that a practical, solvent-free preparation of mononitrotoluene is possible. The reaction mechanism is likely affected by active sites generated on surface of MoO₃ during milling. Both toluene and NaNO₃ molecules are expected to adhere to the active sites and react most effectively when an optimized distribution of the reactants on the surface of the catalyst is achieved.

CHAPTER 3: EFFECT OF PROCESS PARAMETERS ON MECHANOCHEMICAL NITRATION OF TOLUENE²

3.1 Introduction

Nitration of organic compounds is necessary for a wide variety of applications. The majority of energetic materials, for example, are organic compounds with the nitro group as the oxidizer [4]. Nitrated aromatics are also widely used as solvents, dyes [3], pharmaceuticals [5], and perfumes [78]. For energetic materials, nitrotoluene is of particular interest because it is the first precursor in the synthesis of trinitrotoluene or TNT, a common explosive [7, 8]. In addition, nitrotoluene is used in synthesis of toluidine, nitrobenzaldehyde, and chloronitrotoluenes, which are the intermediates for the production of dyes, resin modifiers, optical brighteners and suntan lotions [79]. The nitrating agent for these reactions has traditionally been fuming nitric acid combined with another strong acid, e.g., sulfuric acid, perchloric acid, selenic acid, hydrofluoric acid, boron trifluoride, or an ion-exchange resin containing sulfonic acid groups. These strong acids are catalysts that result in the formation of the nitronium ion, NO₂⁺. Sulfuric acid is most common in industrial nitration because it is both effective and relatively inexpensive.

The common nitration methods have a number of disadvantages. Perhaps most significant is the production of large quantities of spent acid which must be regenerated because its neutralization and disposal on a large scale are environmentally and economically unsound [80]. Another issue is the generation of considerable amounts of environmentally harmful waste during the purification of the products [15]. Additional disadvantages include the hazards associated with handling the nitrating agents, as well as over nitration [16]. The reactions involving strong acids are not selective and yield a mixture of isomers, some of which are less desirable than others. For example, toluene nitration produces a mixture of mononitrotoluene (MNT) isomers with 55-60% of ortho- or o-MNT, 35-40% of para- or p-MNT, and 3-4% of meta-, or m-MNT [79]. This leads to large quantities of unwanted product because the demand for p-MNT is greater than

² A manuscript considered for publication in Journal of Materials Science

for the other isomers [17, 79]. To increase the ratio of p- to o- isomers, nitration is commonly done in the presence of phosphoric acid or aromatic sulfonic acids. While the p/o ratio increases from 0.6 to 1.1-1.5 [79], additional environmentally harmful reactants are used. Another challenge associated with this reaction is the formation of oxidized byproducts. The addition of the nitro group to the aromatic ring of toluene strongly activates its methyl group making it susceptible to oxidation. The oxidation is minimized in industrial toluene nitration by carrying it out at low temperatures [79]. In a batch process, for example, the acids are added at 25°C and the reaction is carried out at 35 – 40°C [79]. The total MNT yield in this reaction is 96% for a batch process, but most patents for continuous processes report yields of up to 50% [79].

Our previous study [81] established the feasibility of mechanochemical nitration of toluene using sodium nitrate as a source of nitronium ions and molybdenum oxide as an environmentally benign catalyst. It was observed that the MNT production was strongly affected by the relative ratios of the starting components, including C₇H₈, NaNO₃, and MoO₃. While MNT was formed, the yield was relatively low and substantial amounts of undesired byproducts formed as well. The reaction mechanism had not been clarified. The objectives of the current work are therefore to, improve the accuracy of product analysis, to identify experimentally the process parameters affecting yield and selectivity of MNT formation, and finally, to interpret the experimental parametric study of MNT production to elucidate the processes and reactions leading to the mechanochemical nitration of toluene.

3.2 Experimental

3.2.1 Sample Preparation

Following our previous work [81], toluene was nitrated by mechanically milling it with sodium nitrate and molybdenum oxide resulting in reaction 2.1. Materials used in the experiments were toluene (Startex, solvent grade), molybdenum oxide MoO₃ (Alfa-Aesar, 99.95 %), and sodium nitrate (Alfa Aesar, 99%). Several milling runs were carried out with a fraction of MoO₃ substituted with silica. Two types of silica were used: fumed silica (Alfa Aesar, 99.8%) and quartz glass obtained by crushing quartz glass cylinders with a hammer and pre-milling it in a shaker mill for 5 minutes. The reactants were milled in a Retsch PM 400MA planetary mill using hardened steel vials and hardened steel balls or glass beads as milling media. The sizes of milling media varied as listed in Table 3.1.

Table 3.1 Milling Media

Media	Diameter
Hardened Steel Balls	1/2" = 12.7 mm
	3/8" = 9.525 mm
	1/4" = 6.35 mm
	1/8" = 3.175 mm
Glass Beads	0.4-0.6 mm (average 0.5 mm)
	0.088-0.149 mm (average 0.125 mm)

The total mass of the solids in each vial was kept constant at 43.3 g, including 1.67 g of sodium nitrate. The volume of toluene was 0.5 ml for most runs, although several samples were prepared with 2 ml toluene. The mass of the milling media was 130 g for all runs, thus the ball to powder mass ratio (BPR) stayed constant at 3. Milling times varied from 0.5 to 4 hrs. All samples were milled at 400 RPM.

In all experiments, the vials were cooled using an air conditioner unit, built into the planetary mill and set at 15.6 °C (60 F). The milling temperature was adjusted further by using custom-made cooling fins (see [82] for details) added to the vials and by employing an intermittent milling protocol. The surface temperatures of the milling vial lids were measured during several runs using previously calibrated thermistors attached to the lids. The readings were taken at half hour intervals throughout the runs. Details of the three temperature control regimes and respective temperatures are listed in Table 3.2. The differences in the vial temperatures associated with the different milling protocols are around 20-25 °C. It is apparent that the milling media had no effect on the vial temperature except for the case of milling with 1/2" steel balls, in which the total number of balls was considerably smaller than in other cases. In the latter case, the temperature was reduced noticeably compared to all other milling media. Additional measurements (omitted from Table 3.2 for brevity) showed that replacing a fraction of MoO₃ with silica had no effect on the vial temperature for any of the temperature control regimes.

Table 3.2 Temperature Control Regimes of Planetary Mill Experiments

Milling balls (media)		Temperature, °C for different milling protocols		
Material	Diameter, inch (mm)	Intermittent milling, fins "Low"	Continuous milling, fins "Intermediate"	Continuous milling, no fins "High"
Glass	0.125 mm		47.3±3.3	
Glass	0.50 mm		44.8±0.2	63.5±3.2
Hardened Steel	1/8 (3.175)	19.0±1.0	47.8±2.9	68.2±5.7
Hardened Steel	1/4 (6.35)	22.3±5.5	47.0±4.4	69.6±2.7
Hardened Steel	3/8 (9.525)		47.3±3.7	
Hardened Steel	1/2 (12.7)		34.2±0.3	42.5±11.7

Based on literature reports of aromatic nitration with fuming nitric acid using MoO₃ on silica support as the catalyst [21], we investigated the possibility of toluene nitration by substituting part of the MoO₃ catalyst with silica. Several 2-hr milling runs were carried out in the planetary mill with varying fractions of MoO₃ replaced with silica. 1/4" hardened steel balls were used as milling media in all of these runs. All three temperature

control regimes listed in Table 3.2 were used with fumed silica; only the intermediate protocol was used with quartz glass.

3.2.2 Sample Recovery

Reaction products were extracted with ethyl acetate (Alfa Aesar, 99.5 %). Before extraction, the milling vials were allowed to cool for 20 minutes by being left in the mill with the air conditioner running. Each milling vial was then opened and 150 ml of ethyl acetate were added to the vial. The vial was closed and placed back in the mill, where it was spun at 300 RPM for 5 min, with balls remaining in the vial, in order to agitate the suspension. This suspension was then stored for further analysis. In two experiments, samples were extracted using a water-cooled 500 ml Soxhlet extractor. The solvent was added into the milling vial and agitated at 300 RPM for 1 minute. The resulting suspension was removed and added into the thimble of the extractor until it was filled. The thimble was then placed in a beaker and kept there until the liquid fraction collected in the beaker. The procedure was repeated until the entire sample was filtered. Then the thimble was placed into the extractor and the solution recovered from the beaker was placed into the extractor flask and boiled for 24 hours with the aid of boiling stones.

3.2.3 Sample Analysis

Each suspension sample was stirred and the solid fraction was separated by centrifuging for 5 minutes in a LW Scientific Ultra-8F centrifuge. The liquid fraction was analyzed in an HP 6890 gas chromatograph (GC, heating profile: 40 °C to 250 °C at 5 K/min; split ratio: 10) coupled with HP G2350A mass spectrometer (MS). Product species were identified using the NIST Mass Spectral Library (NIST 08). Different data processing methods were used to evaluate concentrations of the products using the GC-MS output. In preliminary experiments, as in Ref. [81], the relative yield of MNT, $Y_{MNT,rel}$, was estimated as

$$Y_{MNT,rel} = \frac{\sum P_{MNT}}{P_{Tol} + \sum P_{products}} \quad (3.1)$$

where P indicates the integrated GC peaks, and the subscripts refer to MNT, toluene, and all identifiable products, respectively. Similarly, the relative yield of any of species detected can be estimated by substituting its peak area into the numerator. Using Eq. (3.1) to calculate the product yield introduces several potential errors. In addition to measurement uncertainties, any underestimation of the amounts of toluene and reaction products, whether due to losses or due to the presence of additional products undetected by GC-MS, leads to systematic overestimation of the MNT yield. In order to mitigate some of these uncertainties, the yield was determined relative to the amount of toluene introduced at the beginning of milling. This required calibration of the GC-MS measurements. To achieve that, a known amount of xylene (Sunnyside, solvent grade) was added to the ethyl acetate solution as an internal standard for each subsequent measurement. Figure 3.1 shows a sample GC-MS plot featuring xylene and MNT peaks.

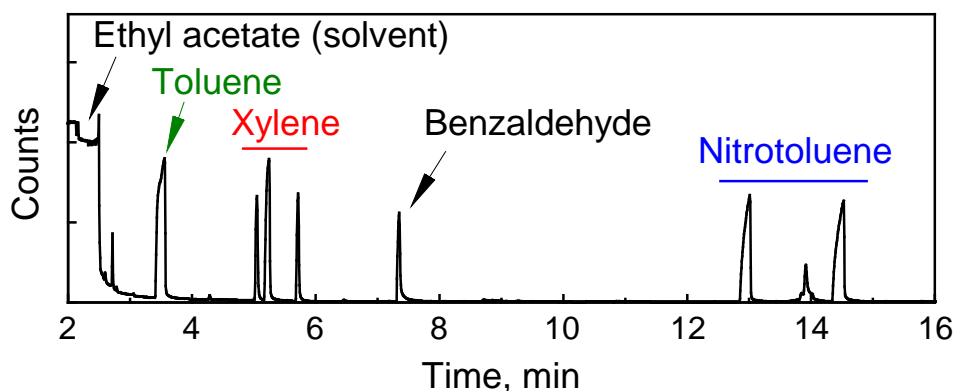


Fig. 3.1 Sample GC-MS trace of a processed sample with xylene added as an internal standard.

In addition to MNT peaks, benzaldehyde (labeled in Fig. 3.1) as well as two dimers: 2-methylphenyl-phenylmethanone and 4-methylphenyl-phenylmethanone (occurring at longer times than included in the figure) were consistently observed as formed byproducts. These species were accounted for when assessing the total recovery of the products of mechanochemical reaction from the milling vials, as discussed below.

The GC peak areas for MNT and toluene were calibrated using reference solutions of toluene, p-MNT (Sigma-Aldrich, 99%), and xylene in ethyl acetate. Actual concentrations could then be determined from the recorded calibration curves and peak ratios of MNT and toluene respectively, to xylene. The absolute yield of MNT, Y_{MNT} , was calculated as

$$Y_{MNT} = \frac{f_{MNT} \left(\frac{\sum P_{MNT}}{\sum P_{xyl}} \right) \cdot C_{xyl}}{C_{tol,0}} \quad (3.2)$$

where f_{MNT} indicates the calibration curve discussed above, P_{xyl} , and C_{xyl} are the peak areas and introduced concentrations of xylene, respectively. $C_{tol,0}$ is the initial toluene concentration at the beginning of milling.

The yield determined using Eq. (3.2) maybe lower than the true yield, because of incomplete recovery of products. Product recovery, R , was therefore assessed by

$$R = \frac{\sum_{products} c_i}{C_{tol,0}} \quad (3.3)$$

where the sum in the numerator contains all toluene-derived species determined by GC-MS, including toluene itself. In this estimate, product species concentrations that were not explicitly calibrated, were estimated by setting their respective calibration function, $f_i(\sum P_i / \sum P_{xyi}) = 1$. This leads to unspecified systematic errors, which can only be corrected if a specific calibration is performed for each species formed. However, the purpose of this analysis is the relative comparison between different runs; therefore, a repeatable systematic error is acceptable.

3.2.4 Surface Area Measurements

Surface area of the solid fraction of several samples was determined using Brunauer–Emmett–Teller (BET) nitrogen adsorption method. After extracting the organic phase, the solid (inorganic phase) was dried and degassed at 350°C for 4.5 hours. After degassing, the surface area of the samples was measured using nitrogen adsorption BET (Quantochrome Instruments Autosorb IQ ASIQM000000-6, 11 point adsorption measurement).

3.3 Results

3.3.1 Preliminary Experiments

In the preliminary experiments, milling times varied from 1 to 4 hours; several kinds of milling media were used; and the relative MNT yield was obtained from Eq. (3.1). Significant relative yields of MNT, in the range of 10% – 90% were observed for all milling conditions, including the experiments with glass beads as the milling media. Comparing the results with different milling media, the lowest yields were observed for 12-mm steel balls. The yields were also relatively low for glass beads. The highest yields were obtained for the milling times of 1-2 hours when 3 – 10-mm diameter hardened steel balls served as the milling media. It was also observed that the recovery of the product using Soxhlet extractor was not more effective than using the solution agitated in the mill; consequently, the latter approach was employed in all experiments discussed below.

3.3.2 Effect of Milling Time and Media

Absolute MNT yield calculated using Eq. (3.2) is shown in Fig. 3.2 for a set of experiments with varied milling times and milling media. The milling protocol employing continuous milling with cooling fins (leading to intermediate vial temperatures, see Table 3.2) was used in all experiments shown. No silica was used. As seen in the figure, the highest MNT yields occur close to 1 hour for runs using 1/4" steel balls as the milling media. Results shown in Fig. 3.2 also suggest that the peak yield may occur at shorter times for 1/8" steel balls, and possibly at longer times for larger steel balls, although additional measurements would be needed to confirm this. For the runs performed with glass beads, the yields were lower than for those with steel balls.

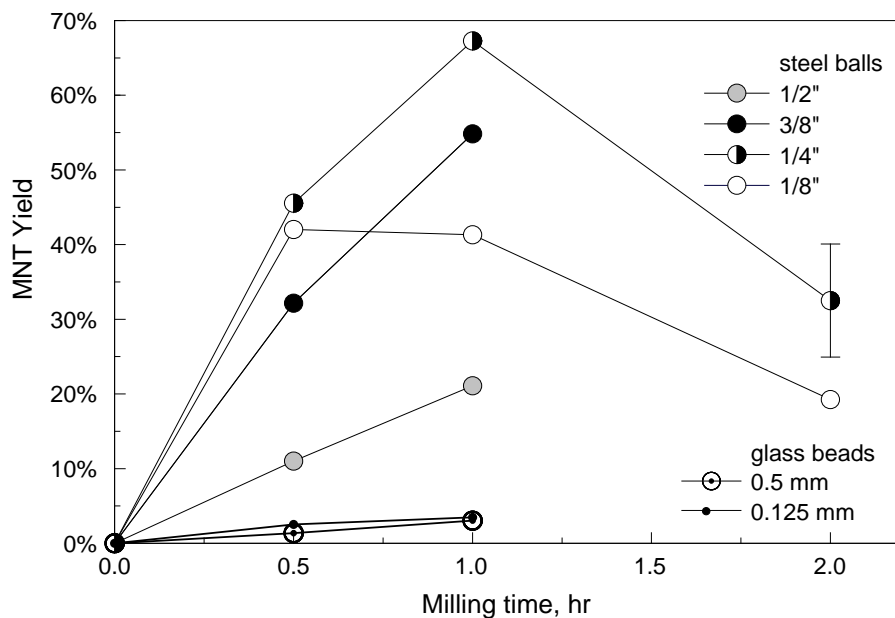


Figure 3.2 Absolute MNT yield for different milling times and milling media. The intermediate temperature regime was used.

To understand the reasons for the reduction in the MNT yield at longer milling times, clearly observed for the cases of 1/8" and 1/4" steel balls, consider data presented in Fig. 3.3. Results for 1/4" steel balls, for which the highest MNT yield was observed, are examined closer. The recovery and MNT yield for that case are compared to the fraction of toluene left in the vial and the fractions of the consistently observed byproducts. All the concentrations were determined by comparing the measured GC-MS peak areas of respective species to that of xylene, while accounting for the actual xylene concentration; then the fraction of each compound was assessed based on the starting amount of toluene, similar to Eq. (3.3). As noted earlier, because no xylene-based calibration was made for the byproducts, the concentrations may include a systematic error. However, the main purpose of introducing such concentrations here is to observe their relative changes as functions of milling time. Therefore, a systematic error is acceptable, as long as all the data is processed consistently. Results in Fig. 3.3 show that most of toluene was consumed by the end of 1-hr milling, when the peak MNT yield was observed. The peak MNT yield occurs at the same time as the peak concentrations of all tracked byproducts. At longer milling times, MNT concentration as well as the byproduct concentrations decrease, while the toluene concentration remains negligible. The reduced recovery at longer milling times could represent either additional reactions in the milling vial, producing products that are not detectable by GC-MS, or physical losses during milling or the extraction procedure.

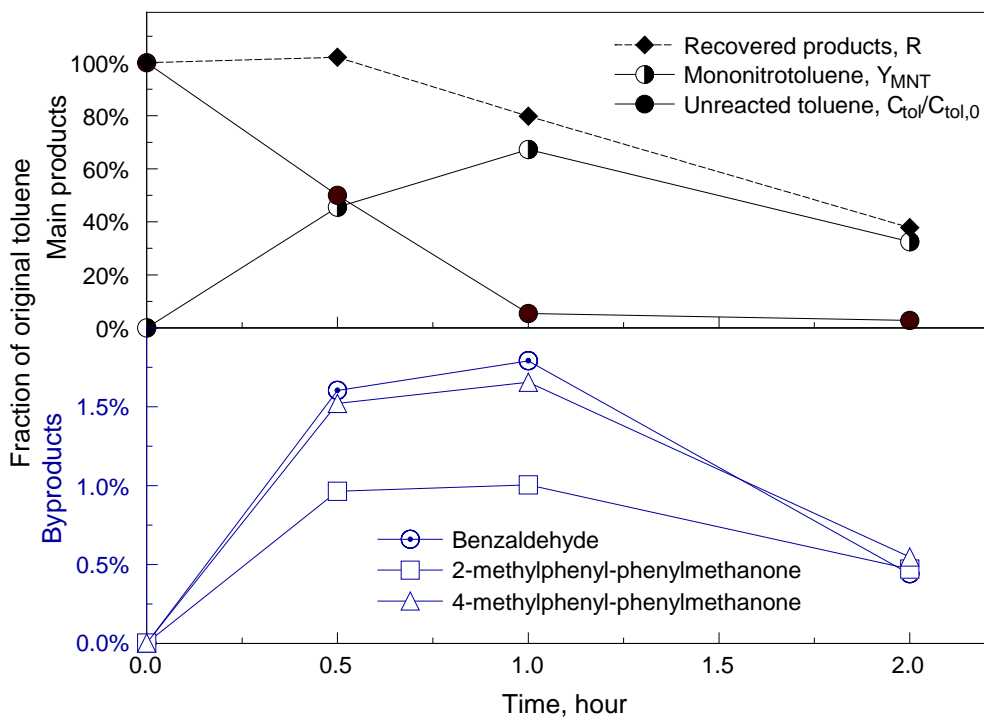


Figure 3.3 Comparison of the total product recovery, absolute MNT yield, and depletion of toluene along with yields of significant byproducts as functions of milling time. 1/4" steel milling balls have been used with the intermediate temperature regime.

3.3.3 Effect of Temperature

Figure 3.4 shows the MNT yield as function of effective milling temperature for 1/4" steel balls, after 2 hours of milling. The error bars show standard deviations from repeat experiments. The overall yield is effectively constant with temperature. The toluene consumption is inversely proportional to the milling temperature, although most of toluene is consumed at all temperatures, consistent with the trends seen in Figure 3.3. However, increased losses at higher temperatures cannot be ruled out. On the other hand, the formation of different byproducts follows different trends. Benzaldehyde is more abundant at low temperatures, while its yield at the higher temperature is reduced. Conversely, the yield of both dimers consistently increases with temperature; a trend opposite to that observed for the total product recovery.

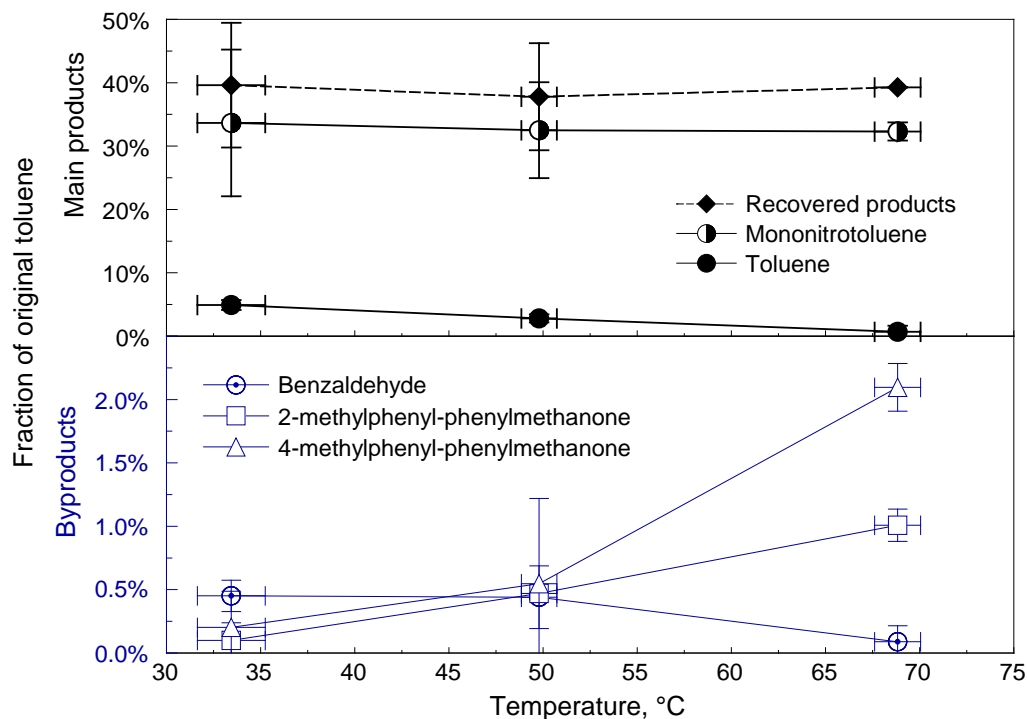


Figure 3.4 Comparison of the total product recovery, absolute MNT yield, and depletion of toluene along with the yield of significant byproducts, as functions of milling temperature. 1/4" steel balls are used. The milling time is 2 hours.

3.3.4 Milling with MoO₃ and Silica

The absolute MNT yield calculated using Eq. (3.3) is shown in Figure 3.5 for multiple experiments performed at a fixed milling time of 2 hours, in which a fraction of MoO₃ was replaced with silica. Different milling protocols resulting in different temperatures were used; both fumed silica and quartz glass were used in different runs. The results show clearly that the MNT yield is highest when about 30 wt % of MoO₃ are replaced with silica. This effect is the same for both fumed silica and quartz glass, although quartz glass gives systematically lower yields than fumed silica. Consequently, the experiments with quartz glass were performed using only one milling protocol. At different temperatures, the maximum yield is observed at about the same fraction of MoO₃ replaced with fumed silica. The lack of a pronounced effect of milling temperature on yield, observed in Figure 3.4 is generally consistent with the results shown in Figure 3.5. For both fumed silica and quartz glass, an increase in the silica content well above 30% causes a substantial reduction in the yield.

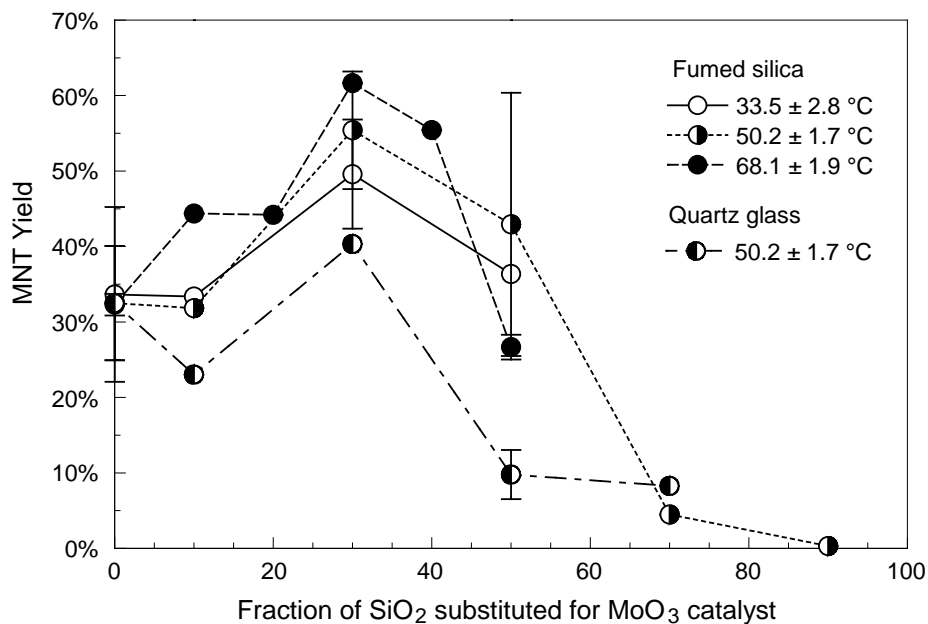


Figure 3.5 Absolute MNT yield vs. fraction of silica replacing MoO₃ for 2-hr runs using 1/4" steel balls as milling media.

In Figure 3.6, the MNT yield is plotted along with the recovery, yields of byproducts, and amount of toluene left for different fractions of silica replacing MoO₃ for the set of experiments with 1/4" steel balls. Initially, both MNT yield and the recovery increase with greater amounts of silica used. Above about 30 % silica, a clear trend of increased toluene concentration (along with the reduced MNT yield) is observed, indicative of an overall lower reaction rate caused by the dilution of the MoO₃ catalyst. The trends observed for byproducts are somewhat different: benzaldehyde forms preferentially at greater silica amounts. Both dimers form with a pattern closely following the formation of MNT. It is interesting that despite greater concentrations of unreacted toluene at high silica amounts, the recovery is relatively low.

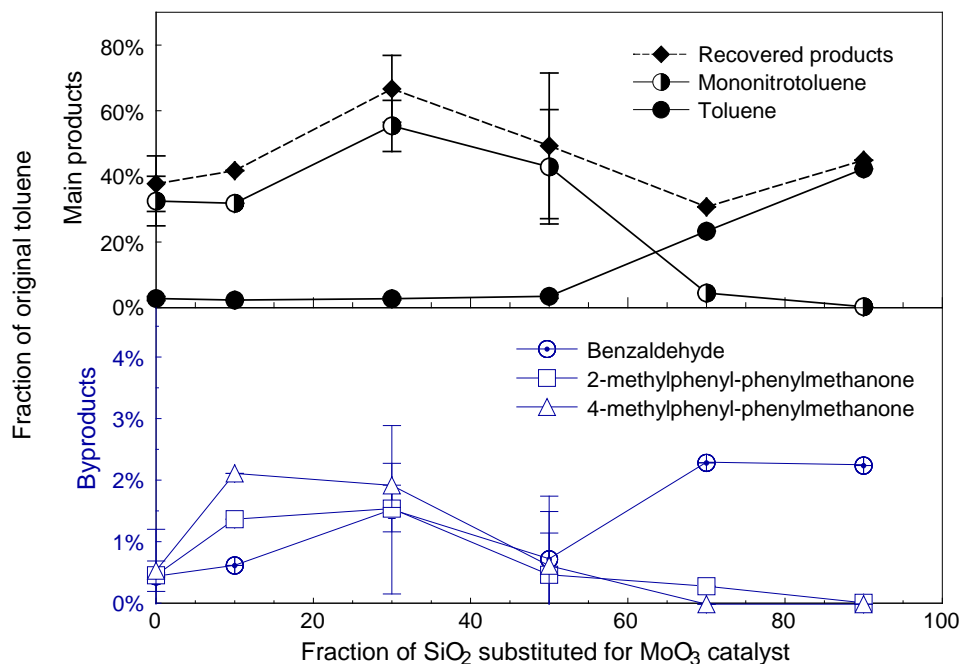


Figure 3.6 Comparison of the total product recovery, absolute MNT yield, and depletion of toluene along with the yield of significant byproducts as functions of the added silica. 1/4" steel milling balls are used with the intermediate temperature milling protocol. Milling time is 2 hours.

Figure 3.7 shows product yields and recoveries vs. temperature for the experiments with 30 % of the MoO₃ catalyst replaced by fumed silica. A weak positive trend in the MNT yield is observed, and as in the case of only MoO₃/no silica, the dimeric byproducts increase with increasing temperature.

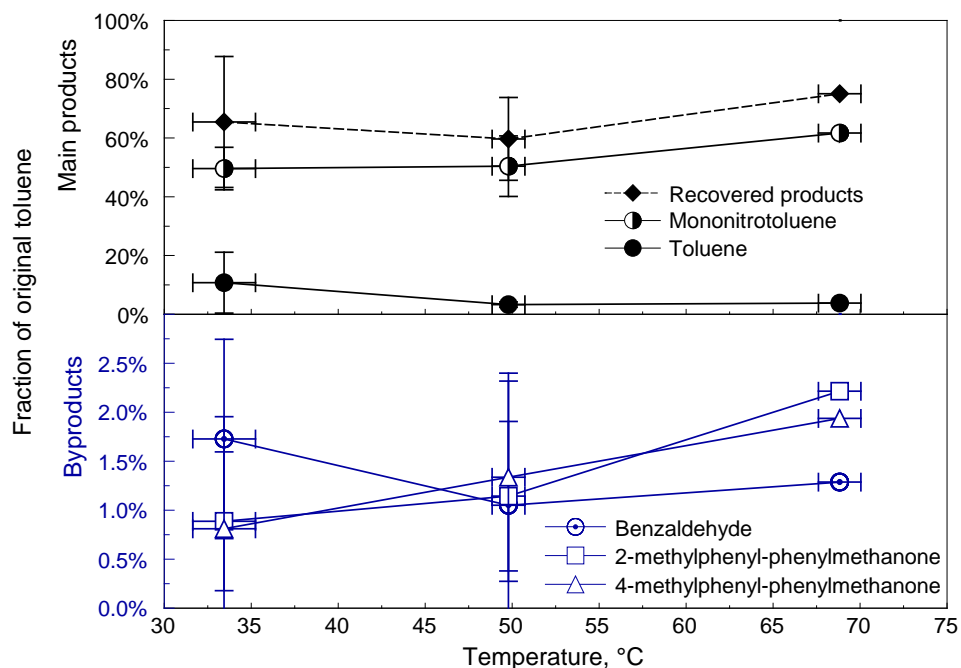


Figure 3.7 Product recovery, absolute MNT yield, and toluene consumption as a function of milling temperature with yield of significant byproducts when 30 % of the MoO₃ catalyst is replaced with fumed silica. 1/4" steel balls are used with the milling time of 2 hours.

3.3.5 Surface Area Measurements

Surface areas of the inorganic fraction of the milled samples were measured for several 2-hr planetary mill runs with varying milling media, with and without silica. For the samples without silica, specific surface areas ranged from 10.4 m²/g to 18.5 m²/g, whereas for the samples milled with 30% silica specific surface areas ranged from 35 to 45 m²/g. The surface area of unmilled fumed silica was determined to be 484 m²/g; thus the surface area of the milled samples was significantly less than the sum of the surface areas of the separate sample components. This indicates that the silica was incorporated with the molybdenum oxide to form composite catalyst particles.

Figure 8 shows the MNT yields determined for a set of 2-hour experiments with corresponding surface area measurements. Results for different milling media and samples with and without 30% SiO₂ substituted for the MoO₃ catalyst have been combined in one plot. The effective milling temperatures are indicated at each data point. There appears to be an overall positive correlation between specific surface area and MNT yield. As shown in Figs. 3.4 and 3.5, MNT yield may also be positively correlated with the milling temperature, although the effect is weak.

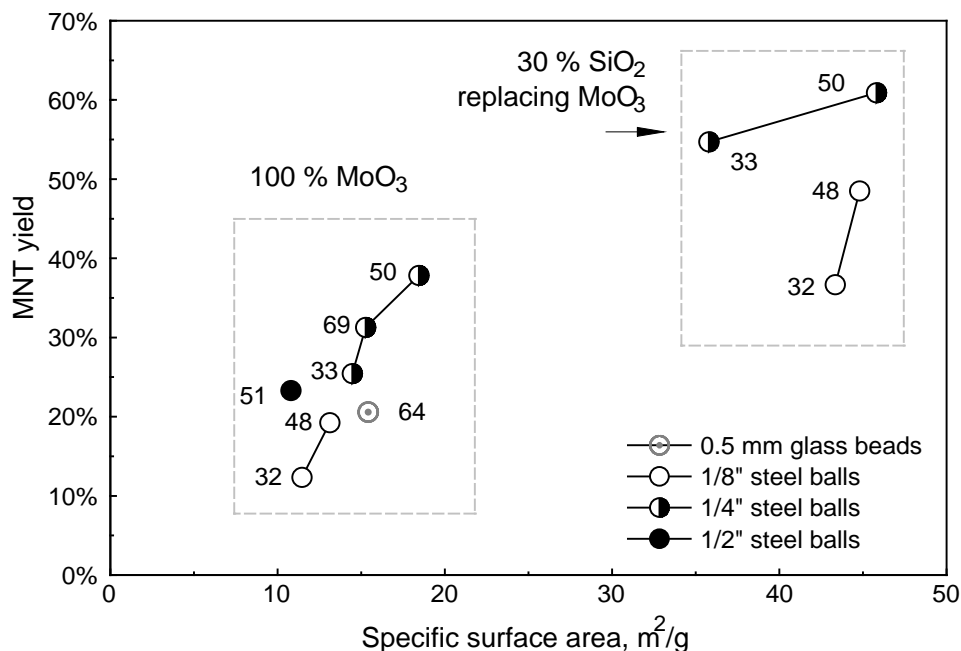


Figure 3.8 Absolute MNT yield as a function of the surface area of the milled solids. Milling time is 2 hours. Data point labels show effective milling temperatures in °C.

3.4 Discussion

In the previous experiments, primarily using a shaker mill [81], it was observed that the reaction yield increased substantially with an increase of solid (catalyst) to liquid (toluene) ratio. The present results, using a planetary mill enabled us to increase considerably the solid to liquid ratio and to achieve respectively higher yields.

Variations in the yield of MNT as a function of different process parameters observed in this study suggest that the mechanochemical reaction of nitration of toluene is relatively complex. As with other mechanochemical reactions, one can initially assume that the reaction rate is proportional to the collision frequency of the milling media; it is further of interest to consider whether the energy dissipated in such collisions is affecting the reaction effectiveness or rate. Finally, it is of interest to consider how the temperature and catalyst properties affect the reaction.

To assess the effect of collision frequency on the reaction rate, consider the results with different milling media sizes shown in Figure 3.2. A possible shift in the maximum yield of MNT to greater milling times for greater ball sizes supports the idea of reaction rate scaling with collision frequency, clearly increasing for smaller balls. However, a reduced absolute maximum yield of MNT for 1/8" steel balls compared to that for 1/4" steel balls suggests that the energy dissipated in collisions affects the reaction effectiveness. The latter conclusion is also consistent with the results of experiments with glass beads. The number of collisions in those experiments was increased greatly; yet, the MNT yield was quite low, suggesting that the reaction does not occur effectively when the collision energies are low.

It is tempting to assign significance to the optimized milling conditions, including milling time of 1 hr (Fig. 3.2) and added 30% of fumed silica (Fig. 3.5) for the yield of MNT observed experimentally. However, the measurements showing the effects of time and silica addition represent both the MNT formation reaction and secondary product formation, or physical losses, as emphasized by the reduced recovery rate seen in Figures 3.3 and 3.6. For the effect of time, in particular (Fig. 3.3), yield of all byproducts and recovery essentially follow each other after the maximum yield is achieved. Importantly, the toluene consumption continues to increase for longer milling times despite the reduced yield of all products. The product recovery reduced at greater milling times, might be caused by greater adsorption of products to MoO_3 particles. The latter could be contributed to modification of MoO_3 surface by the greater number of collisions. Separating the effects of product recovery and optimized yield of MNT needs to be addressed in future work. For example, using solvents other than ethyl acetate employed in the present study may be considered. Alternatively, the reduced recovery rate could be related to secondary products that are not captured by the current extraction technique, such as gases caused by over-oxidation of any of the organic materials.

In case of added silica, the recovery improves with the silica fraction increasing above 70% (Fig. 3.6), while the MNT yield decays, clearly suggesting that it is MoO_3 and not SiO_2 that catalyzes the reaction. Additional experiments at shorter milling times as the most readily controlled experimental parameter may be needed to establish quantitative trends describing the MNT formation alone.

Although the MNT yield and product recovery correlate also for the experiments performed at different temperatures (Fig. 3.4), the yields of both dimers, important reaction byproducts, follow a different trend. An increase in the production of dimers at elevated temperatures suggests a change in the reaction mechanism or an accelerated decomposition of the produced MNT, when the process temperatures are higher. These observations suggest that describing the present mechanochemical reaction theoretically would not be successful if only one global reaction, e. g. reaction 2.1 is assumed. Additional reactions need to be included, which would account for either direct formation of byproducts or for decomposition of the generated MNT.

To consider the effect of added silica on the MNT yield (Fig. 3.5), which was maximized when 30% of silica were added, one may need to account for the combined effect of the remaining catalyst (MoO_3) and an increased surface area of the solid caused by the added silica. The increased surface area is expected to lead to a greater number of mechanically activated reaction events, or greater overall reaction rate. The presence of MoO_3 should account for an effective formation of MNT once the reaction is mechanically activated. It is unlikely that adding relatively small amounts of silica affected significantly the rate of reaction because the peak of MNT yield was observed for the same fraction of silica replacing MoO_3 when different types of silica were used (Fig. 3.5), which were expected to produce different surface areas available for the reaction. The yield peak at about 30% of silica is likely associated with the specific $\text{MoO}_3/\text{SiO}_2$ ratio, which could affect catalytic activity of MoO_3 , e.g., by altering a balance between Lewis and Brønsted acid sites in MoO_3 [83]. It was also reported that silica can interact with MoO_3 and improve its

catalytic activity by forming polymolybdates [21]. Still, another possibility is that the added silica helps generating defects, serving as active sites on MoO₃. The effect of catalyst and its support require further investigation, which can be warranted if the mechanochemical nitration of toluene is to be developed for practical applications.

The relationship between the observed MNT yield, possible reaction mechanism, and the surface area of the solids should also be briefly discussed. Table 3.3 shows selected surface area measurements for 1/8" and 1/4" steel balls with and without 30 % silica, milled in the intermediate temperature regime at effectively 50.2 ± 1.7 °C. Taking the size of the toluene molecule as about 6 Å, derived from its molar volume, the corresponding coverage of the available surface with a toluene monolayer was estimated, and is shown in Table 3.3. A similar estimate is made and shown for MNT as well. The available toluene, if spread uniformly across all solid surface, may form 1-2 monolayers in the cases without silica. It may only form a discontinuous monolayer in the case with silica. In both cases, the estimates suggest that the reaction occurs heterogeneously at the surface in a very thin liquid layer, with properties distinctly different from that of a bulk liquid. The data in Table 3.3 may also suggest that without silica, the available catalyst surface may be rate limiting, while the catalyst surface could be more effectively used with the high-surface area fumed silica added. Note that the formed MNT can only cover a fraction of the available surface and thus is unlikely to result in a substantial reduction in the available catalyst surface. Clearly, such assessments are approximate and combine the toluene present in the milling vial at the beginning of the run with the solid surface measured after the experiment. As the milling run progresses, the amount of toluene decreases. In runs without silica, the solid surface is expected to increase, at least initially; conversely, the surface is decreasing with time in runs with silica present. Despite the general decrease in the surface area in the latter case, the surface of composite MoO₃/SiO₂ particles acting as the catalyst, must be increasing.

Table 3.3 Selected Surface Area Measurements and Surface Coverage Estimates

Sample ID	Ball diameter	silica fraction	SA, m ² /g	surface coverage with toluene monolayer	MNT yield	surface coverage with MNT monolayer
610A	1/8"	0 %	13.1	147 %	19.3%	28 %
610B	1/4"	0 %	18.4	104 %	37.9%	39 %
610C	1/8"	30 %	44.8	43 %	48.5%	21 %
610D	1/4"	30 %	45.8	42 %	60.9%	25 %

3.5 Conclusions

This study has proven that high, practically significant yields of MNT, are attainable by mechanochemical reaction of toluene and sodium nitrate with molybdenum oxide as a catalyst, and without any added solvents. The reaction occurs with a high MNT yield when the ratio of liquid to solid is low, so that toluene is effectively spread in a monolayer on the surface of the catalyst. The rate of the mechanochemical nitration increases with the number of collisions; the reaction efficiency is also strongly affected by the energy dissipated in the collisions. Adding silica to the catalyst MoO_3 increases efficiency of the mechanochemical nitration of toluene as long as a sufficient amount of the catalyst remains available. The results suggest that introducing one global reaction may be inadequate for modeling mechanochemical nitration of toluene. Yields, which were optimized at a specific milling time and with specific silica content, will need to be modeled using additional reactions. Additional reactions are also necessary to describe the observed formation of byproducts, and its dependence on the milling temperature. At low concentrations of catalyst, direct oxidation of toluene by sodium nitrate can generate benzaldehyde, one of the main byproducts. Further work is needed to understand the reason for reduced yield and recovery at longer milling times; use of other solvents or other extraction techniques is necessary.

CHAPTER 4: PRELIMINARY WORK ON NITRATION OF DIFFERENT ORGANIC COMPOUNDS

In addition to the extended effort on nitrating toluene, as discussed above, this study addressed preliminarily nitration of two additional organic compounds illustrated in Fig. 4.1, along with toluene. Feasibility of secondary nitration of toluene was also investigated.

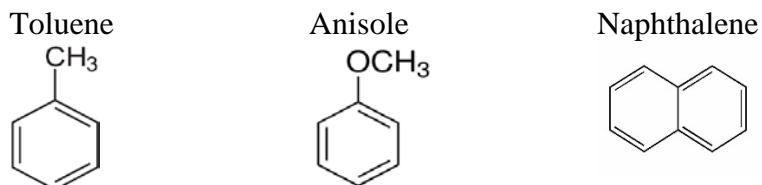


Figure 4.1. Organic compounds nitrated in this study

Experiments with anisole used a planetary mill, ¼” diameter steel balls, and continuous milling with milling fins installed. The solid to liquid loads were similar to those used for toluene. Naphthalene nitration was tested in a shaker mill.

Results of the GCMS analyses of the prepared nitrated compounds are shown in Fig. 4.2. It is apparent that nitrated species are generated in each case, suggesting that the mechanochemical nitration of organic compounds can be developed as a versatile, scalable, and environmentally benign alternative to the current technologies.

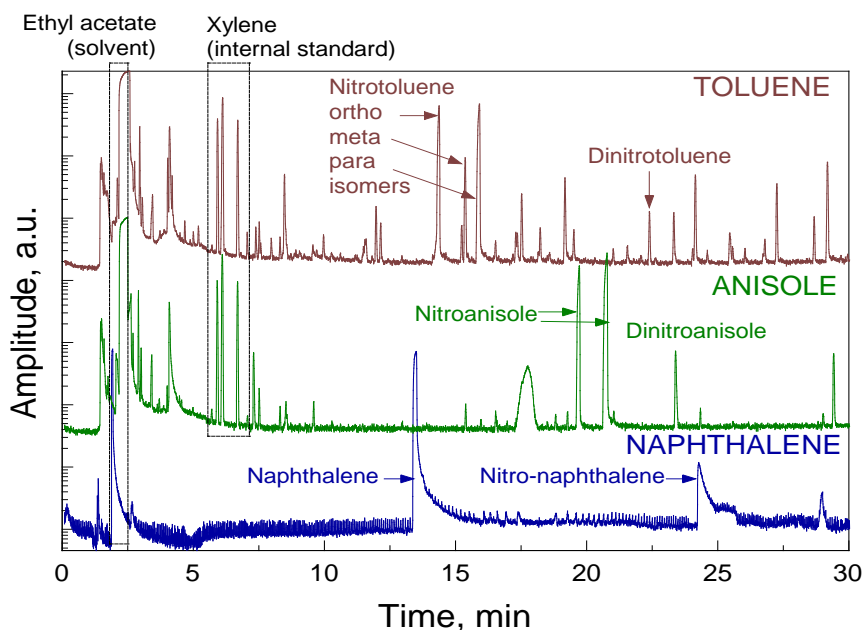


Figure 4.2. GCMS traces for selected mechanochemical experiments on nitration of toluene, anisole, and naphthalene.

CHAPTER 5: CONCLUDING REMARKS

This study investigated mechanochemical nitration of aromatic compounds with a specific focus on the nitration of toluene because of the considerable industrial significance of nitrotoluene. The feasibility of this approach has been clearly demonstrated and practically significant product yields have been obtained. A number of important parameters affecting the desired product yield and selectivity have been identified and studied. These include the ratios of the reactants to each other and to the catalyst, milling time and temperature, milling media size and density. The enhancement of the MoO₃ catalytic activity by adding silica has been explored and the optimum fraction of silica has been identified. The mechanism of this process appears to be complex and still needs to be explored in the future studies, but this study did provide several clues which promise to be useful in that quest. It is interesting that the reaction appears to occur heterogeneously, at the surface of catalyst particles, suggesting a new nitration mechanism observed here.

Potentially, the explored method of nitration of organic compounds is readily scalable and does not require development of new equipment or facilities. Understanding the reaction mechanism would allow one designing process and selecting the process parameters best suited for practical nitration. It is expected varying the catalyst and combining it with a material, which could serve as a molecular sieve, like zeolite, could lead to a substantially better selectivity and thus greater value of the generated nitrated products. It is further necessary to consider possibility of recycling the catalyst, which would significantly improve the value of the new technology.

APPENDIX A: DERIVATION OF THE MILLING DOSE FORMULA

Consider collision frequency by analogy to the collision frequency of molecules given by the molecular theory for collision of molecules in a gas. In that case, the collision frequency is:

$$Z_{ii} = \frac{\sqrt{2}}{2} \pi d^2 \langle c \rangle \left(\frac{N}{V} \right)^2$$

Where d is molecule diameter, N is the number of molecules, V is volume, and c is speed. For the present estimate, the balls can be treated as molecules, so that the d and N are respectively diameter and number of milling balls. Note that balls in the milling vial, unlike molecules in an ideal gas, move together. Thus, multiple collisions involve more than two balls at the same time. This effect is strong, but is not accounted for in the present estimate. The effect becomes stronger as the number of balls increase, while their size is reduced to maintain a constant BPR. Thus, the effect of ball size on the collision frequency is expected to be underestimated.

With this in mind, the milling dose can be expressed as

$$D = Z_{ii} \cdot \left(\frac{mv^2}{2} \right) t$$

$$D \sim d^2 N^2 \cdot \left(\frac{mv^2}{2} \right) t \sim d^2 N \cdot M \cdot t,$$

Where mass of balls $M = N \cdot m$, and the effect of velocity v is removed taking into account that the velocity is driven by the vial motion and thus is the same for all experiments using the same mill. It is further assumed that differences in volume are negligible for different cases.

$$M = Nm = N \cdot \rho \frac{\pi d^3}{6}$$

$$D \sim d^2 N \cdot N \cdot \rho \frac{\pi d^3}{6} \cdot t$$

Number of balls can be taken as $N = \frac{M}{\rho \frac{\pi d^3}{6}}$

Thus

$$D \sim d^2 \frac{M^2}{\rho \frac{\pi d^3}{6}} \cdot t = \frac{M^2}{\rho \frac{\pi d}{6}} \cdot t \sim \frac{M^2}{\rho d} \cdot t$$

Finally, for the same mass of balls,

$$D \sim \frac{t}{\rho d}$$

Considering collective ball motion and significant role of collisions involving simultaneously more than two balls, it is likely that the effect of ball size d is stronger than estimated above.

REFERENCES

1. Topchiev, A.V., *Nitration of Hydrocarbons and Other Organic Compounds*. 2013: Elsevier Science.
2. R. W. Millar, a., et al., *New Synthesis Routes for Energetic Materials Using Dinitrogen Pentoxide [and Discussion]*. Philosophical Transactions: Physical Sciences and Engineering, 1992(1654): p. 305.
3. Schofield, K., *Aromatic Nitration*. 1980: Cambridge University Press.
4. Agrawal, J.P. and R.D. Hodgson, *Organic Chemistry of Explosives*. Organic Chemistry of Explosives. 2007: John Wiley & Sons, Ltd. 1-384.
5. Ono, N., *The Nitro Group in Organic Synthesis*. 2003: Wiley.
6. Jalal Albadi, F.S., Bahareh Ghabezi, Tayebah Seiadatnasab, *Melamine trisulfonic acid catalyzed regioselective nitration of aromatic compounds with sodium nitrate under solvent-free conditions*. Arabian Journal of Chemistry, 2012. **10**: p. S509-S513.
7. Ledgard, J., *The Preparatory Manual of Explosives Fourth Edition*. 2014: Jared B. Ledgard.
8. Akhavan, J., *The Chemistry of Explosives*. 2015: Royal Society of Chemistry.
9. Stamatis, D., et al. *Consolidation of reactive nanocomposite powders*. 2009. Denver, CO.
10. Zukas, J.A. and W. Walters, *Explosive Effects and Applications*. 2013: Springer New York.
11. Williams, D.F. and W.H. Schmitt, *Chemistry and Technology of the Cosmetics and Toiletries Industry*. 1996: Springer.
12. *Nitrobenzene and nitrotoluene*, in *Kirk-Othmer encyclopedia of chemical technology*, J.I. Kroschwitz, Editor. 2004, Wiley-Interscience: Hoboken, N.J.
13. A., C.F., *Organic Chemistry*. 2nd ed. 1992: McGraw-Hill, Inc.
14. Vassena D., K.A., Prins R., *Potential routes for the nitration of toluene and nitrotoluene with solid acids*. Catalysis Today, 2000. **60**: p. 275-287.
15. Meyers, R.A., in *Encyclopedia of environmental analysis and remediation*. 1998, Wiley.
16. Ganjala, V.S.P., et al., *Eco-friendly nitration of benzenes over zeolite- β -SBA-15 composite catalyst*. Catalysis Communications, 2014. **49**: p. 82-86.
17. Peng, X., H. Suzuki, and C. Lu, *Zeolite-assisted nitration of neat toluene and chlorobenzene with a nitrogen dioxide/molecular oxygen system. Remarkable enhancement of para-selectivity*. Tetrahedron Letters, 2001. **42**(26): p. 4357-4359.
18. Adamiak, J.T., W., Skupinski, W., *Interaction of nitromethane with MoO₃/SiO₂ and its influence on toluene nitration*. Catalysis Communications, 2012. **29**: p. 92-95.
19. A. Kogelbauer, D.V., R. Prins, J. N. Armor, *Solid acids as substitutes for sulfuric acid in the liquid phase nitration of toluene to nitrotoluene and dinitrotoluene*. Catalysis Today, 2000. **55**: p. 151-160.
20. Gong, S., et al., *Stable and eco-friendly solid acids as alternative to sulfuric acid in the liquid phase nitration of toluene*. Process Safety and Environmental Protection, 2014. **92**(6): p. 577-582.
21. Adamiak, J., et al., *Characterization of a novel solid catalyst, H₃PO₄/MoO₃/SiO₂, and its application in toluene nitration*. Journal of Molecular Catalysis A: Chemical, 2011. **351**: p. 62-69.
22. Xinhua Peng, H.S., Chunxu Lu, *Zeolite-assisted nitration of neat toluene and chlorobenzene with a nitrogen dioxide/molecular oxygen system. Remarkable enhancement of para-selectivity*. Tetrahedron Letters, 2001. **42**: p. 4357-4359.
23. Pervez, H., et al., *Selective functionalisation. Part 10. The nitration of phenols by pyridine derivatives carrying a transferable nitro group* 1 Part 9. S.O. Onyiriuka and C.J. Suckling, *J. Org. Chem.*, 1986, 51, 1900. Tetrahedron, 1988. **44**(14): p. 4555-4568.

24. Takacs, L., *The historical development of mechanochemistry*. Chemical Society Reviews, 2013. **42**(18): p. 7649-7659.
25. S.L. James, C.J.A., C. Bolm, D. Braga, P. Collier, T. Friščić, F. Grepioni, K.D.M. Harris, G. Hyett, W. Jones, A. Krebs, J. Mack, L. Maini, A.G. Orpen, I.P. Parkin, W.C. Shearouse, J.W. Steed, D.C. Waddell, *Mechanochemistry: Opportunities for new and cleaner synthesis*. Chemical Society Reviews, 2012. **41**: p. 413-447.
26. Boldyrev, V.V. and K. Tkáčová, *Mechanochemistry of solids: Past, present, and prospects*. Journal of Materials Synthesis and Processing, 2000. **8**(3-4): p. 121-132.
27. Friščić, T., *New opportunities for materials synthesis using mechanochemistry*. Journal of Materials Chemistry, 2010. **20**(36): p. 7599-7605.
28. Friščić, T., *Supramolecular concepts and new techniques in mechanochemistry: Cocrystals, cages, rotaxanes, open metal-organic frameworks*. Chemical Society Reviews, 2012. **41**(9): p. 3493-3510.
29. Kaupp, G., *Mechanochemistry: The varied applications of mechanical bond-breaking*. CrystEngComm, 2009. **11**(3): p. 388-403.
30. Baláž, P., *Mechanochemistry in nanoscience and minerals engineering*. Mechanochemistry in Nanoscience and Minerals Engineering. 2008. 1-413.
31. Baláž, P., et al., *Hallmarks of mechanochemistry: From nanoparticles to technology*. Chemical Society Reviews, 2013. **42**(18): p. 7571-7637.
32. Huot, J., et al., *Mechanochemical synthesis of hydrogen storage materials*. Progress in Materials Science, 2013. **58**(1): p. 30-75.
33. Baláž, P., et al., *Chalcogenide mechanochemistry in materials science: insight into synthesis and applications (a review)*. Journal of Materials Science, 2017. **52**(20): p. 11851-11890.
34. Baláž, P., et al., *Mechanochemical Solvent-Free Synthesis of Quaternary Semiconductor Cu-Fe-Sn-S Nanocrystals*. Nanoscale Research Letters, 2017. **12**(1).
35. Côa, F., et al., *Coating carbon nanotubes with humic acid using an eco-friendly mechanochemical method: Application for Cu(II) ions removal from water and aquatic ecotoxicity*. Science of the Total Environment, 2017. **607-608**: p. 1479-1486.
36. Dong, B.X., et al., *Mechanochemical synthesis of CO_x-free hydrogen and methane fuel mixtures at room temperature from light metal hydrides and carbon dioxide*. Applied Energy, 2017. **204**: p. 741-748.
37. Lomovsky, O.I., I.O. Lomovskiy, and D.V. Orlov, *Mechanochemical solid acid/base reactions for obtaining biologically active preparations and extracting plant materials*. Green Chemistry Letters and Reviews, 2017. **10**(4): p. 171-185.
38. Siddhanti, D.A., et al., *The safer and scalable mechanochemical synthesis of edge-chlorinated and fluorinated few-layer graphenes*. Journal of Materials Science, 2017. **52**(20): p. 11977-11987.
39. Takacs, L., *The mechanochemical reduction of AgCl with metals*. Journal of Thermal Analysis & Calorimetry, 2007. **90**(1): p. 81-84.
40. Karolus, M., E. Jartych, and D. Oleszak, *Structure and magnetic properties of nanocrystalline Fe-Mo alloys prepared by mechanosynthesis*. Acta Physica Polonica A, 2002. **102**(2): p. 253-258.
41. Dreizin, E.L. and M. Schoenitz, *Mechanochemically prepared reactive and energetic materials: a review*. Journal of Materials Science, 2017. **52**(20): p. 11789-11809.
42. Dario, B., et al., *Making crystals with a purpose; a journey in crystal engineering at the University of Bologna*. IUCrJ, Vol 4, Iss 4, Pp 369-379 (2017), 2017(4): p. 369.

43. Kaupp, G., M.R. Naimi-Jamal, and J. Schmeyers, *Solvent-free Knoevenagel condensations and Michael additions in the solid state and in the melt with quantitative yield*. Tetrahedron, 2003. **59**(21): p. 3753-3760.
44. Declerck, V., et al., *Solvent-free synthesis of peptides*. Angewandte Chemie - International Edition, 2009. **48**(49): p. 9318-9321.
45. Cheng, X., et al., *Solvent-free synthesis of dihydrofuran-fused [60]fullerene derivatives by high-speed vibration milling*. Chinese Chemical Letters, 2005. **16**(10): p. 1327-1329.
46. Içli, B., et al., *Synthesis of molecular nanostructures by multicomponent condensation reactions in a ball mill*. Journal of the American Chemical Society, 2009. **131**(9): p. 3154-3155.
47. Braga, D., et al., *Mechanochemical preparation of molecular and supramolecular organometallic materials and coordination networks*. Dalton Transactions, 2006. **6**(10): p. 1249-1263.
48. Štrukil, V., et al., *Towards an environmentally-friendly laboratory: dimensionality and reactivity in the mechanochemistry of metal-organic compounds* Electronic supplementary information (ESI) available: PXRD patterns, FTIR spectra and solid-state NMR spectra for selected materials. CCDC 792744 and CCDC 792745. For ESI and crystallographic data in CIF or other electronic format see DOI: 10.1039/c0cc03822a. Chemical Communications, 2010. **46**(48): p. 9191-9193.
49. Todres, Z.V., *Organic Mechanochemistry and Its Practical Applications*. Boca Raton, FL: CRC Press Taylor and Frances Group.
50. Balaz, P., *Mechanochemistry in Nanoscience and Minerals Engineering*. 2008, Berlin: Springer-Verlag.
51. Choksi, T. and J. Greeley, *Partial Oxidation of Methanol on MoO₃ (010): A DFT and Microkinetic Study*. ACS Catalysis, 2016. **6**(11): p. 7260-7277.
52. Tatibouet, J.M., *A Structure-Sensitive Oxidation Reaction: Methanol on Molybdenum Trioxide Catalysis*. Journal of Catalysis, 1981. **72**(2): p. 375-378.
53. Smith, R.L. and G.S. Rohrer, *An atomic force microscopy study of the morphological evolution of the MoO₃ (010) surface during reduction reactions*. Journal of Catalysis, 1996. **163**(1): p. 12-17.
54. Albright, L.F.,
Nitration, in *Kirk-Othmer Encyclopedia of Chemical Technology*. 2000, John Wiley & Sons, Inc.
55. J.G. Hoggett, R.B.M., J.R. Penton, K. Schoefield, *Nitration and aromatic reactivity*. 1971, Cambridge University Press: Cambridge.
56. P.M. Esteves, J.W.D.M.C., S.P. Cardoso, A.G.H. Barbosa, K.K. Laali, G. Rasul, G.K.S. Prakash, G.A. Olah,, *Unified mechanistic concept of electrophilic aromatic nitration: Convergence of computational results and experimental data*. Journal of the American Chemical Society, 2003. **125**: p. 4836-4849.
57. Booth, G., *Nitro Compounds, Aromatic*, in *Ullmann's Encyclopedia of Industrial Chemistry*. 2000, Wiley-VCH Verlag GmbH & Co. KGaA.
58. K.T. Lu, K.M.L., P.C. Lin, K.L. Hwang, *Critical runaway conditions and stability criterion of RDX manufacture in continuous stirred tank reactor*. Journal of Loss Prevention in the Process Industries, 2005. **18**: p. 1-11.
59. M. Zhang, G.H.L., K. Song, Z. Wang, Q. Zhao, S. Li, Z. Ye, *Biological treatment of 2,4,6-trinitrotoluene (TNT) red water by immobilized anaerobic-aerobic microbial filters*. Chemical Engineering Journal, 2015. **259**: p. 876-884.
60. R. Ludwichk, O.K.H., C.P. Kist, A.C. Lopes, T. Cavasotto, D.C. Silva, M. Barreto-Rodrigues, *Characterization and photocatalytic treatability of red water from Brazilian TNT industry*. Journal of Hazardous Materials, 2015. **293**: p. 81-86.

61. S. Tu, F.L., P. Hu, Z. Meng, H. Ran, Y. Zhang, *Preparation of amine-modified silica foams and their adsorption behaviors toward TNT red water*, *Colloids and Surfaces. Physicochemical and Engineering Aspects*, 2015. **481**: p. 493-499.
62. H.R. Pouretedal, S.D., M. Alikhasti, H. Mahmoodi, *Treatment of TNT red water by chemical-modified carbon adsorbent prepared from cheap raw materials of pine tree wood*. *Desalination and Water Treatment*: p. 1-10.
63. R.W. Millar, M.E.C., A.W. Arber, R.P. Claridge, R.M. Endsor, J. Hamid, *Clean nitrations using dinitrogen pentoxide (N₂O₅)-A UK perspective*. *Energetic Materials: Chemistry, Hazards and Environmental Aspects*, 2011: p. 77-106.
64. R.W. Millar, S.P.P., *Clean nitrations: Novel syntheses of nitramines and nitrate esters by nitrodesilylation reactions using dinitrogen pentoxide (N₂O₅)*. *Tetrahedron*, 1997. **53**: p. 4371-4386.
65. P. Holt, G.J., A.J. Sanderson, P. Wesson, J. Worthington, *Development of an Efficient and Green TNT Manufacturing Process, 2004 Insensitive Munitions and Energetic Materials*. 2004, Materials Technical Symposium: San Francisco, CA.
66. A.L. Garay, A.P., S.L. James, *Solvent-free synthesis of metal complexes*. *Chemical Society Reviews*, 2007. **36**: p. 846-855.
67. Kaupp, G., *Mechanochemistry: The varied applications of mechanical bond-breaking*. *CrystEngComm*, 2009. **11**: p. 388-403.
68. Friiċ, T., *New opportunities for materials synthesis using mechanochemistry*. *Journal of Materials Chemistry*, 2010. **20**: p. 7599-7605.
69. Wang, G.W., *Mechanochemical organic synthesis*. *Chemical Society Reviews*, 2013. **42**: p. 7668-7700.
70. L. Ji, C.Q., M. Liu, X. Chen, *Highly Efficient Nitration of phenolic compounds using some nitrates and oxalic acid under solvent free conditions*. *Journal of Chemical Research*, 2011. **35**(2): p. 101-103.
71. Skupiński, W. and M. Malesa, *An infrared study on the MoO₃/SiO₂ catalytic system employed in toluene nitration*. *Applied Catalysis A: General*, 2002. **236**(1-2): p. 223-234.
72. Kemdeo, S.M., V.S. Sapkal, and G.N. Chaudhari, *TiO₂-SiO₂ mixed oxide supported MoO₃ catalyst: Physicochemical characterization and activities in nitration of phenol*. *Journal of Molecular Catalysis A: Chemical*, 2010. **323**(1-2): p. 70-77.
73. Kemdeo, S.M., *MoO₃/SiO₂-ZrO₂ catalyst: Effect of calcination temperature on physicochemical properties and activities in nitration of toluene*. *Bulletin of Chemical Reaction Engineering and Catalysis*, 2012. **7**(2): p. 92-104.
74. Adamiak, J., W. Tomaszewski, and W. Skupiński, *Interaction of nitromethane with MoO₃/SiO₂ and its influence on toluene nitration*. *Catalysis Communications*, 2012. **29**: p. 92-95.
75. T.S. Ward, W.C., M. Schoenitz, R.N. Dave, E.L. Dreizin, *A study of mechanical alloying processes using re-active milling and discrete element modeling*. *Acta Materialia*, 2005. **53**: p. 2909-2918.
76. X. Jiang, M.A.T., M. Schoenitz, R.N. Dave, E.L. Dreizin, *Mechanical alloying and reactive milling in a high energy planetary mill*. *Journal of Alloys and Compounds*, 2009. **478**: p. 246-251.
77. P.R. Santhanam, E.L.D., *Predicting conditions for scaled-up manufacturing of materials prepared by ball milling*. *Powder Technology*, 2012. **201**: p. 401-411.
78. Albadi, J., et al., *Melamine trisulfonic acid catalyzed regioselective nitration of aromatic compounds with sodium nitrate under solvent-free conditions*. *Arabian Journal of Chemistry*, 2012. **10**: p. S509-S513.

79. Dugal, M., *Nitrobenzene and nitrotoluene*, in *Kirk-Othmer encyclopedia of chemical technology*, J.I. Kroschwitz, Editor. 2004, Wiley-Interscience: Hoboken, N.J.
80. Vassena, D., A. Kogelbauer, and R. Prins, *Potential routes for the nitration of toluene and nitrotoluene with solid acids*. *Catalysis Today*, 2000. **60**: p. 275-287.
81. Lagoviyer, O.S., et al., *Mechanochemical Nitration of Aromatic Compounds*. *Journal of Energetic Materials*, 2017: p. 1-11.
82. Umbrajkar, S.M., et al., *Effect of temperature on synthesis and properties of aluminum-magnesium mechanical alloys*. *Journal of Alloys and Compounds*, 2005. **402**(1-2): p. 70-77.
83. Rajagopal, S., J.A. Marzari, and R. Miranda, *Silica-alumina-supported moxide catalysts: Genesis and demise of brønsted-lewis acidity*. *Journal of Catalysis*, 1995. **151**(1): p. 192-203.